東海大學生命科學系

碩士論文

指導教授：謝明麗 博士

Mingli Hsieh, Ph.D

探討碳酸酐酶八號蛋白在 Machado-Joseph disease 的葡萄糖代謝中扮演的角色

The effects of carbonic anhydrase related protein VIII (CA8) on glucose metabolism in Machado-Joseph disease models

研究生：林冠宇

Guan-Yu Lin

中華民國一 0 七年八月

東海大學生命科學系碩士論文

探討碳酸酐酶八號蛋白在 Machado-Joseph disease 的葡萄糖代謝中扮演的角色

The effects of carbonic anhydrase related protein VIII (CA8) on glucose metabolism in Machado-Joseph disease models

研究生：林冠宇

Guan-Yu Lin

指導教授：謝明麗 博士

Mingli Hsieh, Ph.D

中華民國一 0 七年八月

Acknowledgement

算起來在東海生科也過了六個年頭，其中的四年裡，大多數的時間我都在 MH Lab 中度過，選擇在實驗室專心做實驗也意味著放棄了外面多采多姿的世界。即使這段時間過得很累很辛苦，但是也使我獲得了許多，不論是在日常生活中對於待人處事的進退抑或是科學研究上對於實驗問題的探討，希望在將來離開東海之後的日子裡，這些年的努力將使我不會後會當初的決定。

很感謝指導教授謝明麗老師這幾年的諄諄教誨，指導我關於實驗的設計、問題的探討以及對於我邏輯思考的訓練。也很謝謝口委蔡玉真老師與林照雄老師願意撥冗參加我的口試，也給了我很多實用的建議與鼓勵，使得我的論文能夠順利完成。

最後要謝謝經歷過我的實驗室生活的同學、學長姊、學弟妹。這些年來看著周圍的人來來去去，但是在許多年後，我仍然不會忘記實驗室的大家當初的相處、陪伴。與大家一起在 MH Lab 奮鬥的日子也豐富了我的實驗生活。

在取得碩士學位之後，我會發揮我這些年來的所學，迎向外面世界未知的挑戰，不論是在科學的路上繼續砥礪前行，或是進入職場發光發熱，將我的知識應用在對的地方，做出實質的貢獻。

Contents

Abbreviations

Abbreviation	Full name
2-NBDG	2-[N-(7-nitrobenz-2-oxa1,3-diazol-4-yl)-amino]-2-deoxyglycose
ATP	adenosine triphosphate
CA8	carbonic anhydrase 8
DMEM	dulbecco's modified eagle medium
DNA	deoxyribonucleic acid
ECAR	extracellular acidification rate
EGFP	enhanced green fluorescent protein
GLUT	glucose transporter
HEK	human embryonic kidney
HK	hexokinase
HOS	human osteosarcoma
IP_3	inositol trisphosphate
IP_3R1	inositol 1,4,5 trisphosphate receptor type 1
MERRF	myoclonic epilepsy with ragged red fibers
MEM	minimum essential media
ml	milliliter
mM	millimolar
OCR	oxygen consumption
PBS	phosphate buffered saline
PFK	phosphofructokinase
PFKFB	phosphofructokinase/fructose-2,6-biphosphatase 3
shRNA	short hairpin RNA
TIGAR	TP53-inducible glycolysis and apoptosis regulator
µg	microgram

摘要

Machado-Joseph disease（又稱 spinocerebellar ataxia type 3，脊隨小腦共濟失調症第三型)是一種常染色的顯性遺傳的神經退化疾病，屬於多麩醯胺酸(polyglutamine)疾病的一種，在人類第 14 對染色體上的 *MJD* 基因中核甘酸 CAG 不正常的重複造成 ataxin-3 蛋白質具有一段過長的麩醯胺酸(glutamine)序列所導致，這種突變的 ataxin-3 蛋白會在神經細胞中錯誤的折疊、累積，在臨床上會造成小腦萎縮、運動失調與輕度智能障礙等，目前仍然沒有發展出可以完全治療這種疾病的方式。我們實驗室先前的研究證實 CA8 在 MJD 的基因轉殖小鼠中比較野生型有較高的表達。此外，我們之前的結果也顯示在 HEK293-MJD78 細胞株中過度表達 CA8 可以避免不正常的鈣離子釋放並且減少由突變的 ataxin-3 所導致的細胞死亡。有趣的是不論是在 MJD 的病人或小鼠皆有被觀察到顯著的體重下降，表示突變的 ataxin-3 可能會造成代謝方面的缺失。已知神經細胞沒辦法儲存能量，所以神經細胞對於代謝的維持需要大量的葡萄糖作為原料。值得一提的是先前在人類骨肉瘤細胞中 CA8 的下調會顯著降低糖解作用的活性。因此，在這裡我們想要探討 CA8 的表達是否會參與在 MJD 細胞與動物模式所觀察到的代謝缺失中。現有的數據指出在突變的 MJD

存在的情況下包含 glucose transporter 3(GLUT3 以及 phosphofructokinase-1 (PFK1)在內的蛋白表達皆有顯著的下降。在透過 shRNA 下調 CA8 表達的 HEK293-MJD26、HEK293-MJD78、HEK293-MJDt78 三株細胞皆有觀察到 PFK1 在蛋白質表達顯著的下降。此外，在 HEK293-MJD26 的細胞中下調 CA8 的表達會降低 GLUT3 的蛋白質，不過同樣下調 CA8 表達在 HEK293-MJD78 細胞中卻會造成 GLUT3 的上升，在上調 CA8 表達的細胞中 GLUT3 與 PFK1 的表現都會上升。這些發現支持 CA8 在葡萄糖代謝途徑中扮演重要的角色並且在突變 ataxin-3 的存在與否有不同的影響。在過度表達或下調 CA8 的細胞中，進一步透過幾個酵素，包含 phosphofructokinase/fructose-2,6-biphosphatase 3 (PFKFB3)、p53、TP53-inducible glycolysis and apoptosis regulator (TIGAR) 去探討 CA8 與突變 ataxin-3 對於糖解作用調控的影響。我發現在突變 ataxin-3 存在時，導致 PFKFB3 的表達上升，而 TIGAR 的表達卻下降。顯示突變 ataxin-3 造成糖解作用活性降低，使得細胞必須透過調控機制去補償。在改變 CA8 表達時發現，當 CA8 表達改變時，會因為細胞所帶有的正常或突變的 ataxin-3 對於 PKFFB3、p53、TIGAR 有不一樣的影響。未來計畫進一步去探討葡萄糖代謝的中間產物在細胞中的含量，以了解糖解作用的活性在不同細胞株之間的差異。對於 CA8 在 MJD 的葡萄糖代謝途徑中的角色與影響

了解，可以為在 MJD 疾病中針對代謝的治療提供一個可能的目標。

Abstract

Machado-Joseph disease (MJD), also known as spinocerebellar ataxia type 3, is an autosomal dominant neurodegenerative disease. This disorder is caused by an expansion of the CAG triplet within the open reading frame of the *MJD* gene. The mutant ataxin-3 proteins contain a polyglutamine tract, and tend to misfold and aggregate in neuron cells. The clinical symptoms include cerebellar atrophy, loss of motor coordination and mental retardation. Unfortunately, there is still no effective treatment for the disease. Our previous studies demonstrated that carbonic anhydrase protein VIII (CA8) has a significant increase in mRNA and protein levels in MJD transgenic mice as compared with the wild-type mice. In addition, our previous results showed that overexpression of CA8 in HEK293-MJD78 cells may prevent abnormal Ca^{2+} release and reduce cell death induced by mutant ataxin-3. Interestingly, a significant weight loss was observed both in human and mice with MJD, indicating that the mutant ataxin-3 may cause metabolic defects. It is known that neuronal cells are unable to store energy, thus normal metabolic maintenance is dependent on glucose supply. It is noted that down-regulation of CA8 caused a reduction in glycolysis in human osteosarcoma cells. Therefore, in this study I try to

address whether the expression of CA8 is involved in the possible metabolic defects in MJD cellular and animal models. Current data showed that the expression levels of glycolytic enzymes, including glucose transporter 3 (GLUT3) and phosphofructokinase-1 (PFK1), were decreased in the presence of mutant ataxin-3. Knockdown of CA8 by shRNA also down-regulated PFK1 expression in HEK293-MJD26, HEK293-MJD78 and HEK293-MJDt78. Moreover, HEK293-MJD26 cells with downregulated CA8 shewed a decreased expression of GLUT3, but an increased expression of GLUT3 is detected in HEK293-MJD78 cells. Importantly, overexpression of CA8 significant increased GLUT3 and PFK1 in HEK293-MJD78 cells. To gain insight into the regulation of glycolytic pathway, enzymes including phosphofructokinase/fructose-2,6-biphosphatase 3 (PFKFB3), p53 and TP53-inducible glycolysis and apoptosis regulator (TIGAR) were examined. PFKFB3 was increased in cells harboring mutant ataxin-3, whereas TIGAR was decreased in cells harboring mutant ataxin-3, indicating cells with mutant ataxin-3 needed to increase glycolytic activity through the regulating enzymes in order to compensate the reduction in GLUT3 and PFK1. In addition, under the effects of up-regulation or down-regulation of CA8, PFKFB3, p53 and

TIGAR exhibited different responses in the presence of wild-type or mutant ataxin-3. All these findings suggest that CA8 plays an important role in glucose metabolism and has different influences in the presence or absence of mutant ataxin-3. In the future, further investigation should be conducted to verify the cellular levels of some metabolites involved in glycolysis is needed to determine glycolytic activity. To clarify the roles and effects of CA8 in glucose metabolism may provide a potential therapeutics target for metabolic defects in MJD disease.

1. Introduction

1.1 Neurodegenerative disease

Neurodegenerative disease is a progressive loss of function or death of neurons, such as Alzheimer disease, Parkinson disease, Huntington's disease and spinocerebellar ataxia [1-4]. These progressively neurodegenerative disorders are characterized by intracellular or extracellular protein aggregation. Until now, the pathological mechanisms have been gradually revealed as the development of molecular biology. The abnormal processing of the misfolded proteins and defective protein quality control pathway are thought to be the similarities among these disorders [5, 6]. Unfortunately, there is no effective therapeutic avenue to completely cure these diseases. Thus, it is needed to develop therapies to treat or prevent the diseases. Moreover, a better understanding of the regulation of the protein aggregates and the toxic effect of the disease protein may provide biomarkers or therapeutic targets.

1.2 Machado Joseph disease/ spinocerebellar ataxia type 3

Machado joseph disease (MJD)/spinocerebellar ataxia type 3 (SCA3) is an

autosomal dominantly inherited neurodegenerative disease. Genetic pathologies are triggered by the over-repetition of CAG codon in *ataxin-3* gene on chromosome 14q32.1 [7]. The translated proteins, named ataxin-3, have an expended polyglutamine tract and tend to misfold and aggregate in specific neuron cells, resulting in neuronal loss and dysfunction in specific brain regions with particular severity in the cerebellum [8]. Clinical symptoms are characterized by progress ataxia, external ophthalmoplegia, dysarthria and dysphagia [9]. Normal ataxin-3 contains between 13 to 36 times of glutamine repeat, whereas mutant ataxin-3 contains over 55 times of glutamine repeat [7]. Ataxin-3, functions as a deubiquitinating enzyme (DUB), is mainly localized in the cytoplasm and is capable of entering nucleus and interacting with several transcription factors [10].

Expansion of the polyglutamine tracts in the C-terminus likely causes a conformation change in ataxin-3, which may affect many properties of the protein, including stability, interaction with other proteins and tendency to aggregate. Mutant ataxin-3 tends to aggregate in the nucleus [11], and the nucleus compartment is the main site of cellular toxicity in polyglutamine

disease [10]. The intranuclear inclusion (NIIs) is the pathological hallmark in MJD, and the inclusions are revealed to be composed of ubiquitin (Ub) and other proteins such as Ub-like proteins, heat-shock proteins (HSPs), proteasome subunits and transcription factors [12]. Normal ataxin-3 has an intrinsic tend to aggregate through its Josephin domain (JD) in *vitro* and is able to form dimers, even oligomers [4, 13, 14]. The fibrillization of ataxin-3 finally lost its enzymatic activity and made the protein more prone to aggregate [15]. It is worth mentioning that the NIIs abundance is correlated with the number of CAG repeats and disease severity. It is known that several protein quality control pathways have the ability to clear the misfolded and aggregate proteins [16]. However, a protein homeostasis failure was observed in later stage of the disease via MJD transgenic mouse models [17]. A recent study revealed that an autophagosome production decrease causes autophagy impairment in MJD patient-derived fibroblasts [18].

Several caspases and calpains were reported to be responsible for the generation of toxic fragments [19]. Thus, “toxic fragment hypothesis” was proposed for MJD pathogenesis. The aggregation has thought to be

enhanced through the proteolytic cleavage of mutant ataxin-3, and this process generates C-terminus with expanded polyglutamine tract [19-21]. Although wild-type and mutant ataxin-3 undergo the same proteolytic processes, which were conducted by caspases or calpains [22-24], the different stability between wild-type and mutant ataxin-3 may result in different nuclear accumulation rates. Therefore, inhibition of calpains may reduce the accumulation and toxicity both *in vitro* and *in vivo* [25]. However, the stability of C-terminal fragments containing polyglutamine tracts may be different from wild-type and mutant ataxin-3. As C-terminal fragments with the UIM, polyglutamine tracts and NLS (nuclear localization signal) are abundant in the nuclear fraction from MJD patients, but not present in brains from healthy people [19, 26]. Moreover, C-terminal fragments containing NLS favorably accumulate in nucleus, where these fragments can escape from proteolytic degradation conducted by cytoplasmic quality control pathway [27, 28]. Additionally, some chaperon proteins, such as heat shock proteins (HSPs) are known to play a role in folding and maintaining protein structure. It is reported that HSP70 and HSP40 are downregulated in late stage of MJD transgenic mice [17, 23], thus unable to suppress the toxicity of mutant ataxin-3. Meanwhile,

the decreased expression of heat shock protein implying that cellular susceptibility to oxidative stress is increased [24].

Most MJD *in vivo* models are transgenic lines expressing different forms of *MJD* gene, including *M. musculus*, *D. melanogaster*, and *C. elegans* [29-31]. Human yeast artificial chromosome (YAC) constructs containing *MJD* gene with different CAG repeats have been introduced to mice by homologous recombination. The MJD YAC-transgenic mouse models exhibit several symptoms of MJD and have been used to study ataxia and pathologies observed in human MJD patients [32]. Interestingly, the transgenic mice with mutant ataxin-3 show a progressive weight loss and this finding is correlated with the size of CAG repeats and the copy number of *MJD* gene [32]. In addition, the progressive weight loss accompanied with symptoms onset is a common phenotype in MJD patients [29, 33], and the same observation has been found in patients with Huntington's disease [30, 31]. However, the detailed mechanism is still unclear. therefore, we speculate that there are specific metabolic defects associated with polyglutamine diseases.

1.3 Carbonic anhydrase related protein VIII (CA8)

Carbonic anhydrase (CA) has at least five families (α, β, γ, δ and ε), and α-CA is found in mammals. α-CA comprises sixteen isozymes and thirteen (CA1, 2, 3, 4, 5A, 5B, 6, 7, 9, 12, 13, 14, 15) of them have the ability to catalyze the reversible hydration of carbon dioxide (CO_2) to bicarbonate and protons to maintain pH balance in blood. The other three isozymes named carbonic anhydrase-related proteins (CA-RPs), CA8, 10 and 11, are catalytically inactive due to the lack of one or more histidine residues required to bind a zinc ion in their active sites [34, 35]. The exact biological function of CA-RPs is still unclear. Among the three CA-RPs, CA8 specifically expresses in the Purkinje cells of the cerebellum in human and mouse [36, 37]. The expression of CA8 is also observed in organs such as lung and liver [36]. The highly conserved DNA sequence of CA8 indicates that CA8 may have important functions in mammals [38].

Previous studies of CA8 mainly focused on its role in neurodegeneration. A spontaneous mutated *Waddles* mouse, harboring a 19-bp deletion in *CA8* gene, exhibited ataxia and appendicular dystonia [39]. A S100P homozygous point mutation in *CA8* gene has been reported to cause

cerebellar ataxia, mental retardation and quadrupedal gait in Iraqi family [40]. Another point mutation G162R was reported and this CA8 mutation leads to hypometabolic in cerebellar hemisphere and temporal lobes by Fluorodeoxyglucose Position Emission Tomography analysis (FDG-PET) [41], indicating that CA8 may be associated with glucose metabolism. It is noticed that two point mutations S100P and G162R result in a shorter half-life of CA8 protein (Gi *et al*, unpublished data). Furthermore, a novel biochemical function of CA8 was reported to bind inositol 1,4,5-triphosphate receptor 1 (IP3R1) on the endoplasmic reticulum and decrease the binding affinity of IP3 [36]. Our previous study indicated that down-regulation of CA8 in cybrids cell lead to a significant increase of ATP-induced calcium release [42]. These findings given the fact that CA8 may play an important role in modulation of intracellular calcium signaling. Interestingly, the abnormal calcium release was thought to be associated with the pathogenesis of MJD [43], and this aberrant cellular calcium signaling was caused by mutant ataxin-3 through the interaction with IP3R1 [44]. The results suggest that the expression of CA8 may provide neuroprotective function by suppressing abnormal calcium release.

1.4 CA8 and cancer

Cancer related studies also revealed that CA8 was abundantly expressed in non-small cell lung cancer and colorectal cancer [37, 45, 46]. Increased expression of CA8 is associated with cancer cell growth and invasion ability in colorectal carcinoma [45]. It is known that normal cells generate energy through oxidative respiration in mitochondrion. However, cancerous cells produce energy mainly by high rate of glycolysis even in the presence of oxygen [47]. This metabolic transition is tightly linked to AKT signaling pathway [48]. Therefore, possible anticancer therapeutics were proposed through the inhibition of glycolytic activity [49, 50]. Our previous findings in human osteosarcoma cells have demonstrated that CA8 not only enhances cell invasion and cell viability but also significantly affects glycolytic activity was also observed in HOS cells [51]. Moreover, a decreased level in p-AKT (phosphorylated AKT) was observed in HOS cells with CA8 knockdown, indicating an oncogenic role of CA8.

1.5 CA8 and neurodegenerative disease

Recent studies in our laboratory have revealed that downregulation of CA8 in zebrafish results in defective motor control and abnormal calcium

release [52]. Additionally, a significant decrease in CA8 mRNA and protein expression has been observed in cells containing MERRF A8344G mutation in mitochondrial DNA (mtDNA). Myoclonus Epilepsy with Ragged-Red Fibers (MERRF) syndrome is a mitochondrial disease with pathological features of myoclonus, generalized epilepsy and ataxia. It was then demonstrated that overexpression of CA8 in MERRF cells decreases cell death under staurosporine (STS) treatment, suggesting a protective role of CA8 in MERRF cells harboring A8344G mutation in mtDNA [42]. Furthermore, STS treatment on neuronal cells with up-regulated CA8 also exhibited a decreased cell death, indicating a protective function of CA8 in neuronal cells [52]. In addition, c*a8* morpholino zebra fish showed an affected motor reflection revealed an important role of CA8 in motor control [52]. An elevation in glucose uptake ability was also observed in neuronal cells and MJD cerebellar granule neurons with CA8 overexpression (Li *et al*, unpublished data). Interestingly, compromised glucose uptake was also reported in HD mice models [53]. Huntington's disease (HD), another well-known polyglutamine disease, also has a CAG over-repetition in *huntingtin* gene. It was reported that HD and MJD have similar mechanism in aggregation formation and pathogenesis [3, 54]. The

limited glucose uptake may be one of the possible mechanisms in metabolic abnormality. Moreover, some key enzymes involved in glycolysis, such as glucose transporter 1 (GLUT1) and glucose transporter 3 (GLUT3), showed a reduced protein expression in patients with early stages of HD [55]. An impaired GLUT3 trafficking underlies the glucose hypometabolism in HD was observed in HD mice [56]. In addition, the protein of phosphofructokinase, which is responsible for the conversion from fructose-6-phosphate to fructose-1, 2-phosphate, is decreased in protein expression level in caudate and putamen of HD [57].

Previous studies in our laboratory indicated that CA8 may interact with mutant ataxin-3 in MJD disease models (Li *et al*, unpublished data). Therefore, in this study we aimed to understand the roles of CA8 in the regulation of glycolytic pathway in the presence of mutant ataxin-3 both *in vivo* and *in vitro*, and to dissect the possible metabolic defects in MJD.

2. Material and method

2.1 Cell lines

Human neuroblastoma cell line SK-N-SH (HTB-11; ATCC) was provided by Dr. Shin-Lan Hsu (Taichung Veterans General Hospital, Taiwan) and human embryonic kidney cell line HEK293 (CRL-1573; ATCC) was provided by Dr. His-Chi Lu (Tunghai University, Taiwan). SK-N-SH was cultured in Dulbecco Modified Eagle Medium supplemented with 1% non-essential amino acid (Corning), 2mM L-glutamate (Corning), 1U/ml penicillin-streptomycin (Corning), 10% fetal bovine serum (Gibco), and HEK293 was culture in Minimum Essential Medium supplemented with 1U/ml penicillin-streptomycin (Corning), 10% fetal bovine serum (Gibco).

2.2 Animals

MJD84.2 MJD transgenic mice harbor a YAC transgene that expresses two copies of human ataxin-3 gene with an expanded 84 CAG repeats and their wild type littermates C57BL/6J were provided by Dr. Chin-San Liu (Changhua Christian Hospital, Taiwan). Mice were maintained on a 12hr light/dark cycle and given ad libitum access to food and water. All of the

mouse-use protocols in this research were approved by the Institutional Animal Care and Use Committee.

2.3 Plasmid construction

peGFP-N1-MJD26 contains full-length ataxin-3 with 26 CAG repeats, peGFP-N1-MJD78 contains full-length 78 ataxin-3 with CAG repeats and peGFP-N1-MJDt78 is lack of N-terminus of ataxin-3 (deletion of amino acids 20-244) were constructed by Wei-Hsiu Chang [24]. pcDNA3.1-HA-MJD78 contains full-length ataxin-3 with 78 CAG repeats was kindly provided Dr. Henry Paulson. The recombinant DNA sequence was confirmed by DNA sequencing. A lentiviral vector contains full-length CA8 with myc tagged (pLKOAS3w.puro.CA8myc) was amplifying by PCR and CA8myc DNA sequence was inserted between *N*heI and *EcoRI* of pLKOAS3w.puro. The control lentiviral vector eGFP (pLKOAS7w.eGFP.puro), shRNA expression lentiviral vector of shCtrl (pLKO.1-shLuc, TRCN72249) and shCA8 (TRCN000153276) were purchased from the National RNAi Core Facility.

2.4 Cell culture and selection of stable cells

HEK293 cells were maintained in MEM (Minimum Essential Medium) and transfected with peGFP-N1-MJD26, peGFP-N1-MJD78, peGFP-N1-MJDt78. Stable cells were selected in culture medium contained with 500 ug/ml G418 (Geneticin, GIbco). HEK293 cells stably expressed MJD26, MJD78, and MJDt78 were infected with lentiviruses carrying recombinant pLKO.1 shLuc, pLKO.1 shCA8, pLKOAS7w.eGFP.puro, pLKOAS3w.CA8myc.puro, which of all were generated by National RNAi Core Facility. Infection protocol of modified virus for stable expression or knockdown of CA8 was performed according to the instructions provided by the National RNAi Core Facility. SK-N-SH cells were maintained in DMEM (Dulbecco Modified Eagle Medium) and transfected with pcDNA3.1-MJD78HA. Stable cells were selected in culture medium contained with 500 ug/ml G418 (Geneticin, GIbco). SK-N-SH cells stably expressed MJD78HA were infected with lentiviruses carrying recombinant pLKOAS7w.eGFP.puro, and pLKOAS3w.CA8myc.puro. Expression of CA8 were determined by Western blot analysis using anti-CA8 antibody. Selection of stable cells was performed to culture cells in medium contained with 1ug/ml puromycin (Sigma) for 5 days. Cells will be collected after

another 10 days. Cells were transfected using TOOLSmoothFect transfection reagent (BIOTOOLS). Transfection was performed with 2ug of plasmids and followed by the manufacturer's instructions. After 48 hours, cells were selected in culture medium contained with 500 ug/ml G418 (Geneticin, GIbco). Stable cells were collected after 21 days. Expression of GFP or HA were analyzed using Western blot and stained with anti-GFP or anti-HA antibody.

2.5 Preparation of protein lysates for SDS-PAGE

Mouse cerebellum tissues were resuspended in 200 ul of RIPA buffer (50mM HEPES-KOH, 150mM sodium chloride, 1mM sodium EDTA, 1mM sodium EGTA, 1% NP-40, 0.7% sodium deoxycholate, 0.1% SDS, 15% glycerol) and homogenized on ice. Cells were washed third times with PBS and resuspended in 100ul of RIPA buffer. After incubated on ice for 1 hour, protein lysates from tissues or cells were sonicated on ice for 15min, then centrifuged at 13000rpm for 30min at 4^{o}C. The supernatant was collected and protein concentration was determined by using Bio-Rad protein assay kit (Bio-Rad laboratories).

2.6 Western blot

The cell lysates containing 30ug of protein were load in 10% sodium dodecyl sulfate (SDS) polyacrylamide gels. The resolved proteins were electrophoretically transferred to 0.2 um PVDF membrane. After blocking the membrane with TTBS (10 mM Tris-HCl pH7.5, 150 mM NaCl, and 0.1% Tween-20) containing 5% non-fat milk or 5 % BSA for 1hr in room temperature. Primary antibody binding was performed by incubating the PVDF membrane with proper antibody titers according to data sheet for overnight at 4°C. The membranes were then incubated with secondary antibody conjugated with HRP (Horseradish peroxidase) for overnight at 4°C. Signals were detected by the enhanced chemiluminescent (Millipore). Protein bands were quantified by densitometry and normalized with α-tubulin or β-actin. For quantification of proteins, the amount of protein loaded on the gel was optimized, and multiple exposures were performed to ensure that the signals were within the linear response range.

2.7Glucose uptake

SK-N-SH cells were seeded at the density of 1.3×10^5 cells/well in Falcon

96-well black plate with clear bottom and incubated for overnight at 37°C, 5% CO_2 incubator. After a 4 hr starvation in medium without glucose and FBS, cells were then incubated with glucose free medium supplemented with 300uM 2-[N-(7-nitrobenz-2-oxa1,3-diazol-4-yl)-amino]-2-deoxyglycose (2-NBDG) (Life technologies) for 1 hr. After washed three times with PBS, the fluorescence of 2-NBDG was recorded at 37°C in the SpectraMax M2e Microplate Reader (Molecular Device) at the excitation wave length of 465 nm and the emission wavelength of 540 nm.

2.8 Immunofluorescence

Cells were seeded on glass coverslips at 1×10^5 in 24 well tissue culture plates and incubated at 37°C in 5% CO_2 incubator overnight. After the cells were attached, cells were washed three times with PBS (pH7.4), fixed with 4% paraformaldehyde (PA) in PBS for 20 min at room temperature. Cells washed PBS were then blocking using 10% fetal bovine serum (FBS) with PBST (PBS containing 0.05% Triton X-100) for 1 hr at room temperature. The samples were incubated with the primary antibody for overnight at 4°C (anti-GFP 1:200, anti-ataxin-3 1:200, anti-GLUT3 1:200, anti-CA8 1:200).

After washed with PBST, the samples were then incubated with secondary antibodies conjugated with DyLight 649 or alex fluoro 488 (Jackson ImmunoResearch) for 2 hr at room temperature. Finally, samples were washed and mounted. The images were detected using Zeiss LSM 880 confocal microscope.

2.9 Immunoprecipitation

Mice cerebellums were solubilized in RIPA buffer (50mM HEPES-KOH, 150mM sodium chloride, 1mM sodium EDTA, 1mM sodium EGTA, 1% NP-40, 0.7% sodium deoxycholate, 0.1% SDS, 15% glycerol) and lysates were cleared by centrifugation. 500 ug proteins were incubated with magnetic beads (Invitrogen) to clear non-specific binding proteins. After separated by magnet, proteins were incubated with primary antibody (antibody titers were used according to data sheet) for 6 hr at 4^{o}C. The protein-antibody complexes were isolated by magnet, and the complexes were then incubated with magnetic beads for overnight at 4 ^{o}C. Finally, the beads were pelleted by magnetic and washed with washing buffer (50 mM Tris-HCl, pH 7.9, 150 mM NaCl, 1 % NP-40, 1.5 mM MgCl2, 1 mM EGTA, 1 mM EDTA). The immunopellets were resuspended in SDS-PAGE sample buffer and subjected

to electrophoresis and Western blot analysis.

2.10 Statistics

Protein bands in figures were quantified by densitometry using Image J and values were expressed as ± SEM. Analysis of the difference between groups was performed with Student's t-test. p-values smaller than 0.05 were considered statistically significant.

3. Results

3.1 Proteins expression of ataxin-3 and CA8 in SK-N-SH and HEK293 cells

Our previous data demonstrated that both protein and mRNA expression levels of CA8 are higher in human neuroblastoma cells expressing mutant ataxin-3 compared with cells expressing wild-type ataxin-3 [58]. In addition, the results from immunochemical staining showed that CA8 protein expression is increased in the cerebellum of MJD84.2 transgenic mice in contrast with wild-type control (Fig. S1). This increase may result from the increased transcriptional activity of *carp8* gene (Fig. S2). Therefore, stable cell lines, previously established in our laboratory, were used in the following experiments, including HEK293-MJD26 (HEK293 cells expressing MJD gene with 26 CAG repeats), HEK293-MJD78 (HEK293 cells expressing MJD gene with 78 CAG repeats) and HEK293-MJDt78 (HEK293 cells expressing MJD gene with N-terminal truncated 78 CAG repeats) [59]. Western blot showed wild-type and mutant ataxin-3 expression in theses cell lines (Fig. 1C and Fig. 1D). The expression of mutant ataxin-3 in SK-N-SH was shown as Fig. 1G. To further investigate the role of CA8 in

MJD cellular models, we established cell lines expressing different levels of CA8 through lentivirus infection. After antibiotic selection, stable clones included HEK293-MJD26-shLuc, HEK293-MJD78-shLuc, HEK293-MJDt78-shLuc (HEK293 infected with Luc-shRNA), HEK293-MJD26-eGFP, HEK293-MJD78-eGFP (HEK293 infected with pLKOAS7w.eGFP), HEK293-MJD26-shCA8, HEK293-MJD78-shCA8, HEK293-MJDt78-shCA8 (HEK293 infected with lentiviral shCA8 to knockdown CA8), HEK293-MJD26-CA8myc, HEK293-MJD78-CA8myc (HEK293 infected with pLKOAS3w.puro-CA8-myc), SK-N-SH-HAMJD78-eGFP (SK-N-SH-HAMJD78 infected with pLKOAS7w.eGFP), SK-N-SH-HAMJD78-CA8myc (SK-N-SH-HAMJD78 infected with pLKOAS3w.puro-CA8-myc) cells were established for the following experiments. Western blot analysis showed that CA8 protein expression was significantly decreased after CA8 down-regulation and increased after CA8 overexpression (Fig. 1E and Fig. 1F). Overexpression of CA8 was also detected in SK-N-SH-HAMJD78-CA8myc (Fig. 1H).

3.2 The ability of glucose uptake is reduced in the presence of mutant ataxin-3

Knowing that neuronal glucose metabolism is correlated with brain activity [60], I speculated that the ability of neuronal cells to uptake glucose seems to be important to polyglutamine disease. As metabolic defects are well described symptoms of polyglutamine diseases, including Huntington's disease and SCA1 [61, 62], it is possible that glucose uptake is declined in cells expressing mutant ataxin-3. To measure glucose uptake in different cells as well as in primary neurons, 2-[N-(7-nitrobenz-2-oxa1,3-diazol-4-yl)-amino]-2-deoxyglycose (2-NBDG) were used for the glucose uptake assay in the SK-N-SH MJD cellular models [59], and primary neurons of MJD84.2 transgenic mice. Previous data from our laboratory indicated that cerebellar primary neurons with mutant ataxin-3 displayed a significant decrease in glucose uptake compared with their wild-type control neurons (data not shown). However, down-regulated or overexpressing CA8 in cerebellar primary neurons from wild-type mouse showed no significant difference in glucose uptake (Fig. S3). In this study, it was revealed that the glucose uptake rate was decreased in SK-N-SH cells expressing mutant ataxin-3 as compared with that of parental cells, while overexpression of CA8 in SK-N-

SH-HAMJD78 cells exhibited a significant increase in glucose uptake (Fig. 2). Taken together, our results showed that cells expressing mutant ataxin-3 had a reduced ability of glucose uptake and this deficiency can be rescued in cells with CA8 overexpression.

3.3 The expression of glycolytic enzymes is decreased in cells expressing mutant ataxin-3

It is known that a significant body weight loss was reported in MJD84.2 transgenic mice [63]. Consistent with this observation, MJD patients have lower body mass index without loss of appetite [33]. To explain the underlying mechanism, some studies have proposed a possible defective glucose metabolism in polyglutamine diseases [61, 64, 65]. It is known that two isozymes of GLUTs, GLUT1 and GLUT3, are specifically expressed in cerebellar neurons [66]. Thus, we first examined the protein expression of these two transporters in MJD cellular model (Fig. 3A and Fig. 3B). As shown in Fig. 3B, the protein expression of GLUT3 was significantly decreased in HEK293 cells harboring polyglutamine expanded ataxin-3, and a more dramatic decrease was observed in cells with truncated mutant ataxin-3 (Fig. 3B and Fig.3F). However, GLUT1 expression showed no difference

among these cell lines (Fig. 3A).

After glucose is transported into cells, it is then undergone a ATP-dependent-phosphorylation by hexokinase (HK) to form glucose-6-phosphate (G6P). Therefore, two of the hexokinase isozymes were examined in our studies. HKI is known to be the major isozyme expressed in the brain [67], and another isozyme HKII has a neuroprotective function and may slow down neurodegeneration [68]. In our studies, HKI and HKII protein expression was analyzed in HEK293 cells expressing either wild-type or mutant ataxin-3. As shown in Fig. 3C, protein expression of HKI tended to decrease in HEK293 cells expressing both full-length and truncated mutant ataxin-3. However, there is no significant difference in protein levels of HKII among HEK293-MJD26, HEK293-MJD78 and HEK293-MJDt78 (Fig. 3D). Therefore, we next focused on phosphofructokinase-1 (PFK1), which catalyzes the phosphorylation of fructose-6-phosphate (F6P) to fructose-1,6-bisphosphate (F1,6BP) [69]. Western blot analysis showed that protein expression of PFK1 was significantly reduced in HEK293 cells with polyglutamine expanded ataxin-3 (Fig. 3E and Fig. 3F). Quantitative analysis revealed a significant decrease of PFK1 in HEK293-MJD78 and

HEK293-MJDt78 as compared with that in HEK293-MJD26 cells. Taken together, our results indicated that significantly decreased GLUT3 and PFK1 in the presence of mutant ataxin-3 may lead to attenuated glycolysis.

3.4 Decreased expression of glycolytic enzymes in cells with down-regulated CA8

Previous study has revealed that human osteosarcoma cells with down-regulated CA8 displayed a decrease in both glycolytic activity and ATP synthesis [51], indicating that CA8 may play an important role in glucose metabolism. To further determine whether the expression of CA8 leads to an alteration in glycolytic enzymes, Western blot analysis was conducted in HEK293 MJD cellular models with different expression levels of CA8. Our results showed that the protein levels of HKI and HKII have no difference in HEK293 MJD cell lines with different expression of CA8 (Fig. 4B and Fig. 4C). On the other hand, our data demonstrated that GLUT3 expression is decreased in HEK293-MJD26-shCA8 as compared with the shLuc control cells. However, down-regulated CA8 resulted in an increased GLUT3 expression in HEK293 cells containing both full-length and truncated mutant ataxin-3 (Fig. 4A). We further investigated whether knockdown of CA8 has

any influence on the protein expression of PFK1 in HEK293 cells harboring wild-type or mutant ataxin-3 (Fig. 4D). The results showed that PFK1 protein expression was decreased in HEK293-MJD26, HEK293-MJD78 and HEK293-MJDt78 with down-regulated CA8, indicating that CA8 knockdown may result in a reduction of glycolytic flux. Furthermore, in order to investigate whether overexpression of CA8 would lead to a reverse effect caused by reduced expression of CA8. The protein expression of GLUT3 and PFK1 were examined in HEK293 MJD cellular models. Our results revealed that both GLUT3 and PFK1 protein expression did not altered in HEK293-MJD26 and HEK293-MJDt78 cells overexpressing CA8 (Fig. D and Fig. E). However, up-regulation of CA8 significantly increased the protein level of PFK1 in HEK293-MJD78 cells (Fig. 4E and Fig. 4J). In summary, up-regulation or down-regulation of CA8 may cause changes in expression of GLUT3 and PFK1, and these effects are associated with ataxin-3.

3.5 CA8 is co-localized with GLUT3 in MJD transgenic mice and cellular models

It was previously demonstrated that decreased glucose uptake and glycolytic

activity were observed in HOS cells with CA8 down-regulation [51]. In addition, our above mentioned data revealed that CA8 down-regulation leads to altered protein expression of GLUT3. Therefore, we speculated that CA8 may be involved in glucose uptake and there may exist a protein-protein interaction between CA8 and GLUT3. We first examined the distributions of CA8 and GLUT3 in MJD transgenic mice by immunofluorescence. The results revealed that CA8 was partially co-localized with GLUT3 in Purkinje cells of the cerebellum from wild-type and MJD transgenic mice (Fig. 5A). However, this co-localization did not show significant alteration in cells with and without mutant ataxin-3. We then examined the cellular distribution of CA8 and ataxin-3 in HEK293-MJD26 and HEK293-MJD78 cells. The results showed a partially co-localization of CA8 and ataxin-3 in MJD cellular models (Fig. 5B). The signals of co-localization of either CA8 and GLUT3 or CA8 and ataxin-3 distributed unevenly within the cellular compartment. However, the presence of mutant ataxin-3 did not show any effects on the protein distribution of both CA8 and GLUT3.

3.6 CA8 interacts with GLUT3 in the presence or absence of mutant ataxin-3

To further confirm the possible interaction between CA8 and GLUT3, we next determined the protein-protein interaction of CA8, GLUT3 and ataxin-3 by immunoprecipitation. Our results showed a protein-protein interaction between endogenous CA8 and GLUT3 by using protein lysates from the cerebellums of wild-type and MJD transgenic mice (Fig. 6A and Fig. 6B), supporting that CA8 may regulate glucose import via interacting with GLUT3. Interestingly, the interaction seemed to be stronger in MJD transgenic mice as compared with that in the wild-type mice (Fig 6B), but the binding affinity of CA8 to GLUT3 remains to be clarified. Taken together, the protein-protein interaction exists among CA8, ataxin-3 and GLUT3 may provide a possible explanation for the mechanism that CA8 and mutant ataxin-3 are involved in the glycolytic pathway.

3.7 CA8 regulates glycolytic pathway through PFKFB3 and TIGAR

Since PFK1 is one of the important enzymes involved in glycolytic pathway, it is tightly controlled by several activators and inhibitors. It is known that fructose 6-phosphate (F6P) can be converted to fructose 2,6-

bisphosphophate (F2,6BP) which is reported to be the allosteric activator of PFK1 [70] (Fig. S7). The phosphorylation is catalyzed by phosphofructokinase 2 (PFK2), the most potent activator eliminating the allosteric activation of F2,6BP to PFK1 [70]. Thus, the abundance of PFK2 and the cellular concentration of F2,6BP is critical to the regulation of PFK1 activity. Because phosphofructokinase/fructose-2,6-biphosphatase 3 (PFKFB3), one isozyme of PFK2, is mainly involved in neuronal glycolysis [71], we first measured the expression level of PFKFB3 in our cellular model. As shown in Fig. 7A, HEK293 cells expressing full-length mutant ataxin-3 did not show a difference in protein expression of PFKFB3 as compared with HEK293 cells with wild-type ataxin-3. However, a significantly increased protein expression of PFKFB3 was detected in HEK293 cells expressing truncated mutant ataxin-3 (Fig. 7A and Fig. 7B). Meanwhile, it is known that the phosphorylation of F2,6BP is a reversible reaction and the dephosphorylation of F2,6BP is regulated by TP53-inducible glycolysis and apoptosis regulator (TIGAR). Therefore, we examined the protein expression of TIGAR and p53 in HEK293 MJD cellular model. Though our data showed a significant reduction in protein level of TIGAR in HEK293 cells expressing mutant ataxin-3 as compared to that in HEK293 expressing

wild-type ataxin-3 (Fig. 7A and Fig. 7D), no differences in p53 protein expression were observed in HEK293 cellular models. On the other hand, knockdown of CA8 did not cause a change in protein expression of PFKFB3 in HEK293 cells with wild-type or full-length mutant ataxin-3 (Fig. 7E, Fig. 7G, Fig. 7H and Fig. 7I), but down-regulated CA8 resulted in a significant decrease in p53 protein level in HEK293 cells expressing mutant ataxin-3 (Fig. 7E, Fig, 7K and Fig, 7L). Moreover, the protein expression of TIGAR exhibited a significant reduction in HEK293-MJD78-shCA8 and HEK293-MJDt78-shCA8 as compared with their shLuc control (Fig. 7E, Fig. 7N and Fig, 7O). Additionally, overexpression of CA8 led to significantly decreased protein expression of PFKFB3 and p53 in HEK293-MJD78 (Fig. 7F, Fig. 7H and Fig. 7K), while CA8 up-regulation did not cause changes in HEK293-MJDt78 cells (Fig. 7F, Fig. 7I, Fig. 7L and Fig. 7O). Taken together, down-regulated CA8 does not affect PFKFB3, p53 and TIGAR in HEK293 expressing wild-type ataxin-3. However, altered protein expression of CA8 may cause different effects on PFKFB3 and TIGAR in HEK293 cells harboring full-length or truncated mutant ataxin-3.

4. Discussion

Previous results from our laboratory demonstrated that mRNA and protein levels of CA8 were raised in human neuroblastoma cells harboring mutant ataxin-3 [58] and an increase of CA8 protein expression was observed in Purkinje cells of MJD transgenic mice by immunohistochemistry staining (Fig. S1). These results indicated that mutant ataxin-3 may contribute to the increase of CA8 expression. In addition, it was reported that a progressive weight loss was observed in MJD patients and transgenic mice despite without loss of appetite [29, 32], and this body weight drop was correlated with the size of CAG repeats [33]. These observations suggested that metabolic defects may be common features of MJD. Interestingly, our previous findings showed that knockdown of CA8 resulted in decreased glucose uptake and glycolytic activity in human osteosarcoma cells [42], supporting that CA8 is involved in glucose metabolism. Therefore, we hypothesized that metabolic defects caused by MJD may be associated with CA8 expression. To clarify the molecular mechanism behind the metabolic impairment observed in MJD patients, three human embryonic kidney cell lines stably expressing normal ataxin-3 (MJD26), mutant

ataxin-3 (MJD78) and N-terminal truncated mutant MJD (MJDt78) were previously established in our laboratory and were used for the current study [24]. In this study, I first examined ataxin-3 protein expression in these three cell lines. Western blot analysis showed the expression of wild-type or mutant ataxin-3 can be detected by antibody against either ataxin-3 or GFP (Fig. 1C and Fig. 1D). However, mutant ataxin-3 can only be detected by antibody against GFP because the epitope for antibody against ataxin-3 is between amino acid F112-L249, which was truncated from MJDt78 (Fig. 1A). SK-N-SH MJD cellular model was previously established and described [59]. Signals from mutant ataxin-3 was detected as shown in Fig. 1G. Furthermore, overexpressed CA8 was fused with a myc tag and shown in Fig. 1H. Because the lack of endogenous CA8 in parental SK-N-SH cells, the signals cannot be observed via Western blot (Fig. 1H).

To determine the possible effects of mutant ataxin-3 on glucose metabolism, I first investigated the ability of glucose uptake in SK-N-SH MJD cellular model. My results from glucose uptake assays showed that a significant decreased glucose uptake in SK-N-SH cells expressing mutant ataxin-3 was observed (Fig. 2), implying that the presence of mutant ataxin-3 caused

an attenuated glucose uptake and may subsequently reduce glucose metabolism.

In order to examine the underlying mechanisms of the metabolic defects involved in MJD, Western blot analysis was performed to analyze a few downstream enzymes on glycolysis. Knowing that the first step of glucose catabolism is the uptake of glucose from extracellular environment, I examined two major GLUTs in the brain, glucose transporter 1 and glucose transporter 3 (GLUT1 and GLUT3) [72]. My results revealed that cells containing mutant ataxin-3 showed a significant decrease in protein expression of GLUT3 and a further reduction in GLUT3 protein level can be observed in HEK293-MJDt78 (Fig. 3B and Fig. 3F). It is noted that the truncated fragment of mutant ataxin-3 causes more cytotoxicity [19, 22], which may be resulted from the severe reduction in GLUT3 protein expression. However, I did not observe any difference in protein expression of GLUT1 in cells with or without mutant ataxin-3 (Fig. 3A), which may be due to the most ubiquitous expression of GLUT1 in mammalian tissues. In addition, GLUT1 is thought to be barely affected by external stimulation [73], and account for basal cellular glucose uptake [74], which may explain

the consistent expression of GLUT1 even in the presence of mutant ataxin-3. It is known that GLUT1 and GLUT3 expression is decreased in early stage of Huntington's disease [55]. Increased copy number of GLUT3 was found to ameliorate pathogenesis and prolong lifespan in a Drosophila model of Huntington's disease [75]. Our results supported the notion that GLUT3 may play an important role in the pathogenesis of polyglutamine disease.

To gain insight into the effects of mutant ataxin-3 on the downstream molecules of glycolysis, hexokinases (HKs) were then investigated. HKs phosphorylate glucose transported by GLUTs to produce glucose-6-phosphate (G6P). There are four HK isozymes in mammals and two of them were well-studied. One is HKI, which is the major isozyme expressed in the brain [67], and the other isozyme HKII is known to promote neuronal survival and may slow down neurodegeneration [68, 76]. HKI and HKII are ubiquitously expressed in mammalian tissues and located on mitochondrial outer membrane. The mitochondrial bound HKI and HKII facilitates the coupling of glycolysis and oxidative phosphorylation [77], which is defective in Huntington's disease [78]. In addition,

overexpression of HKII in Parkinson's disease mouse models prevented neuronal cell death, as well as reduced the associated motor defects [76]. In my study, protein expression of HKI seemed to be decreased in HEK293-MJD78 and HEK293-MJDt78 (Fig. 3C). However, this reduction was not observed in HEK293 cells with transiently expressed mutant ataxin-3 (data not shown). On the other hand, HKII protein expression showed no difference in MJD cellular models (Fig. 3D). I do not know yet the reasons for the differential expression of HKI and HKII in MJD cellular models, but the altered expression of HKI and HKII in stable cells may need to be confirmed in primary neurons from MJD transgenic mice.

I then investigated the expression of phosphofructokinase-1 (PFK1), which catalyzed the phosphorylation of fructose-6-phosphate (F6P) to fructose-1,6-bisphosphate (F1,6BP). It is worth mentioning that PFK1 is a rate-limiting enzyme and important to mediate glycolytic flux [79, 80]. My results showed a significant decrease of PFK1 in HEK293 cells expressing full-length and truncated mutant ataxin-3 (Fig. 3E and Fig. 3G). Consistently, overexpression of PFK1 prevents loss of photoreceptor in Huntington's disease Drosophila models [81]. In addition, the expression

of PFK1 is associated with neuronal differentiation [82]. The activity of PFK1 was reported to sustain neuronal synaptic function and behavior [83]. Therefore, we speculate that the decreased expression of PFK1 in the presence of mutant ataxin-3 may result in the impairment of neuronal differentiation via glycolytic defect. Because the high-energy demand property of neuronal cells, the restrictions on energy supply may cause negative effects on neuronal function and survival. However, whether the activity of PFK1 is altered in cells harboring mutant ataxin-3 remained to be verified.

Meanwhile, in order to investigate the effects of CA8 expression in MJD cellular model, SK-N-SH-HAMJD78, HEK293-MJD26, HEK293-MJD78 and HEK293-MJDt78 stably expressing different levels of CA8 were established. First, we examined the effects of CA8 on glucose uptake in SK-N-SH MJD cellular model. The results from glucose uptake showed that CA8 overexpression led to a significantly increased glucose uptake as compared with SK-N-SH cells expressing mutant ataxin-3, but did not show a statistical significance as compared with SK-N-SH parental cells (Fig. 2). It is worth noting that overexpression of CA8 tended to increase

glucose uptake in cerebellar primary neurons from MJD transgenic mice (Fig. S3B). The similar observation of CA8 in glucose uptake was reported in our previous study of HOS cells [51]. Meanwhile, previous results indicated that down-regulated or overexpressing CA8 in wild-type cerebellar primary neurons showed no influence on glucose uptake (Fig. S3A). Taken together, these results suggest that it is possible that CA8 rescues the defects in glucose uptake caused by mutant ataxin-3 and is involved in glucose metabolism.

Western blot analysis of the effects of CA8 on the glycolytic enzymes, which were investigated previously was then conducted. As shown in figure 4A, GLUT3 protein expression was significantly decreased in HEK293-MJD26 with down-regulated CA8. Although protein expression of GLUT3 tended to increase in HEK293-MJD78 and HEK293-MJDt78 with down-regulated CA8 (Fig. 4A). Knockdown of CA8 led to an increased GLUT3 expression in the presence of mutant and truncate ataxin-3 may suggest a complementary effect due to the cytotoxicity of polyglutamine tracts. However, this tendency is not statistical significance, so more biological repeats are still needed. Moreover, CA8 overexpressed

in HEK293-MJD78 increased protein expression of GLUT3, but CA8 did not cause the same effect on HEK293-MJDt78, which may give an explanation to the rescued glucose uptake in SK-N-SH-HAMJD78 with up-regulated CA8. Notably, it is possible that CA8 expression is involved in the membrane distribution of GLUTs, and the expression of GLUTs may be increased in the presence of mutant ataxin-3 to facilitate more glucose imported from extracellular environment. It is well-known that GLUTs transport monosaccharides only when they are localized on the cell membrane [84], supporting that the process of the re-distribution of GLUTs was important for their normal function. Moreover, a defect on Rab11-mediated membrane translocation of GLUT3 is reported in Huntington's disease [56]. The function of glucose transporter is thought to be related to the disease progression of Alzheimer's disease [85]. However, more investigations for the relationship among CA8, ataxin-3 and the cellular distribution of GLUTs are needed.

Meanwhile, in order to validate the relationship among CA8, GLUT3 and ataxin-3, we further investigated the cellular distributions of CA8, GLUT3 and ataxin-3. Immunofluorescence staining from cerebellum frozen section

revealed a partial co-localization between CA8 and GLUT3 in Purkinje cells of both 52 week-old wild-type and MJD transgenic mice (Fig. 5A). It was noted that CA8 was mainly distributed in the cytoplasm, where it co-localized with GLUT3. However, the localization of CA8 and GLUT3 did not alter in MJD transgenic mice. As shown in Figure 5B, CA8 was co-localized with ataxin-3 in HEK293 cells. Again, the cellular distribution of GLUT3 was not affected by mutant ataxin-3. Although mutant ataxin-3 altered the expression of both CA8 and GLUT3 (Fig. 3F and Fig. 3G), it did not cause a cellular re-distribution of these molecules. Even though insulin treatment was reported to promote neuronal glucose uptake via the translocation of GLUT3 [86], we did not observe the same results in an attempt to treat HEK293t cells with insulin (data not shown). It is possible that the membrane distribution of GLUT3 cannot be detected under the current experimental conditions. In summary, whether the existence of mutant ataxin-3 plays a role on the cellular distribution of glucose transporter remains to be confirmed.

In this study, we further reported a protein-protein interaction between CA8 and GLUT3 by the use of cerebellar lysate from 52 week-old wild-type or

MJD transgenic mice (Fig. 6A and Fig. 6B). It is noted that a recent study in our laboratory revealed an interaction between CA8 and ataxin-3 by immunoprecipitation in the SK-N-SH and HEK293 MJD cellular models. Unfortunately, this interaction was not confirmed by using cerebellar lysates from MJD transgenic mice. It is possible that the amount of endogenous CA8 is insufficient to bring down the weakly interacted mutant ataxin-3 (Li *et al*, unpublished data). In this study, the protein-protein interaction between CA8 and GLUT3 seemed to be stronger in the presence of mutant ataxin-3 (Fig. 6B), evidenced by more GLUT3 brought down by CA8 under the same experimental conditions, suggesting that mutant ataxin-3 may enhance the interaction between GLUT3 and CA8. However, whether the interaction between CA8 and GLUT3 is direct or indirect remains to be addressed.

On the other hand, knockdown or overexpression of CA8 made no effects on the expression of HKI and HKII (Fig. 4B and 4C), indicating that CA8 may not be involved in the expression of HKs in MJD. However, we cannot exclude the possibility that the activity of HKI and HKII is affected by CA8. Interestingly, knockdown CA8 in HEK293 cells with either wild-type or

mutant ataxin-3 showed a significant decrease in the protein expression of PFK1 (Fig. 4D), and is statistically significant (Fig. 4I and Fig. 4J). It is worth noting that mRNA level of PFK1 was significant decreased in MJD transgenic mice (Fig. S4). Given the fact that wild-type or mutant ataxin-3 did not alter the decreased PFK1 expression which was resulted from CA8 down-regulation, it is possible that down-regulated CA8 is sufficient to cause a dramatic reduction of PFK1, suggesting that CA8 is important to glycolytic activity. In addition, overexpression of CA8 caused a significant increase of PFK1 protein expression only in HEK293-MJD78, supporting the results of GLUT3. It means the altered expression of CA8 may affect glycolytic flux by mediating the expression of several glycolytic enzymes. Our previous study reported that HOS cells with down-regulated CA8 resulted in a significant reduction in extracellular acidification rate (ECAR), implying an impaired glycolytic activity. Knockdown of CA8 also led to an decrease in phosphorylated AKT (pAKT), which was reported to mediate glycolysis and energetic stability [87]. However, in the MJD cellular model, the underlying mechanism of CA8 in glycolytic pathway is still needed to be addressed.

It is known that PFK1 is important in glycolytic pathway and there are several activators and inhibitors that tightly control PFK1 activity [88]. PFK1 catalyzes the conversion of fructose 6-phosphate (F6P) to fructose 1,6-bisphosphophate (F1,6BP), whereas the other isozyme, PFK2, phosphorylates F6P to fructose 2,6-bisphosphophate (F2,6BP). The allosteric activation of F2,6BP to PFK1 increases the binding affinity of F6P and overrides the ATP inhibition of PFK1 [70]. Thus, PFK2 is one of the most potent activators of glycolysis [70]. In addition, phosphofructokinase/fructose-2,6-biphosphatase 3 (PFKFB3) is an isoform of PFK2 which specifically expresses in neurons and is committed in neuronal glycolysis [71]. It is reported that PFKFB3 regulates autophagy through AMPK activation [89]. Autophagy impairment is one of hallmarks in MJD patients [18, 90]. Moreover, Meclizine, a compound that enhances glycolysis through PFK2, showed neuroprotective function in Parkinson's disease as well as Huntington's disease [91, 92]. My results showed no difference in protein expression of PFKFB3 between HEK293 cells expressing wild-type or full-length mutant ataxin-3, but a significant increase of PFKFB3 was detected in HEK293-MJDt78 (Fig. 7A and Fig. 7B). On the other hand, no difference of p-AMPK (Thr172) was observed

in HEK293 MJD cellular models with down-regulated CA8 (data not shown). Moreover, knockdown of CA8 failed to affect the protein level of PFKFB3 (Fig. 7E, Fig. 7G, Fig. 7H and Fig. 7I). Nevertheless, a significant decreased PFKFB3 expression was observed in HEK293-MJD78 with overexpressed CA8 (Fig. 7F and Fig/ 7H). It was reported that PFKFB3 has a much higher kinase activity than phosphatase activity while the other PFKFBs have similar kinase and phosphatase activity [93], suggesting that PFKFB3 mainly functions in producing F2,6BP and enhances glycolytic flux [80]. In summary, the presence of full-length mutant ataxin-3 and the down-regulation of CA8 do not cause any effects on the expression of PFKFB3. Importantly, overexpressed CA8 decreases protein level of PFKFB3 in HEK293-MJD78, indicating that in the presence of full-length mutant ataxin-3, CA8 may enhance glycolysis by increasing the expression of GLUT3 and PFK1 directly, and thus inhibits the regulating effects of PFKFB3. To confirm this possibility, more studies on the cellular concentration of F1,6BP and F2,6BP may be required.

It is well-known that the dephosphorylation of F2,6BP is mainly conducted by TP53-inducible glycolysis and apoptosis regulator (TIGAR).

Expression of TIGAR lowers the cellular concentration of F2,6BP, thus inhibits glycolysis [94]. Moreover, TIGAR expression was shown to have neuroprotective function against oxidative stress [95, 96], which may be involved in the pathology of polyglutamine diseases [24, 97, 98]. In my studies, TIGAR showed a significant decrease in HEK293-MJD78 and a more dramatic reduction can be observed in HEK293-MJDt78 (Fig. 7A and Fig. 7D). Noting that PFKFB3 is significant increase in HEK293-MJDt78, it means that under the toxicity of truncated mutant ataxin-3, cells need to up-regulated glycolytic flux through PFKFB3 and TIGAR in order to compensate the reduced expression of GLUT3 and PFK1. In addition, down-regulated CA8 showed a decreased expression of TIGAR in HEK293-MJD78 and HEK293-MJDt78, whereas up-regulated CA8 caused no effects on HEK293 MJD cellular models (Fig. 7E, Fig. 7F, Fig. 7N and Fig. 7O). The influence of CA8 on TIGAR was only exist in cells with mutant ataxin-3, indicating that cells expressing mutant ataxin-3 is supposed to increase glycolytic through TIGAR while CA8 is down-regulated. However, we did not detect a significant change of p53, the upstream regulator of TIGAR, in HEK293 cells expressing mutant ataxin-3 (Fig. 7A and Fig. 7C). Moreover, knockdown of CA8 showed decreased

p53 expression only in HEK293 cells harboring mutant ataxin-3. Besides, a more significant decrease was only observed in HEK293-MJD78 with CA8 overexpressed (Fig. 7F and Fig. 7K). It is noted that other study in our laboratory showed a significant reduction in protein levels of p53 in HEK293t with transiently down-regulated CA8 (Fig. S5). p53, a well-known factor in mediating apoptosis, may regulate glycolytic rate through the mediation of TIGAR [94]. Additionally, p53 was revealed to prevent neuronal death from acute toxicity and maintain cellular redox homeostasis by regulating mitochondrial function [99, 100]. p53 appears to play a pivotal role in the development of neurodegenerative diseases through its interaction with several cellular factors [101]. Polyglutamine related studies also indicated that expression level and activity of p53 are associated with the pathological progression of polyglutamine diseases [102]. It is noted that p53 undergoes the ubiquitin-proteasome degradation pathway [103], which is mediated by ataxin-3. Indeed, mutant ataxin-3 regulates the stability and apoptotic function of p53 [104]. Recent studies indicated that neuronal death triggered by mutant ataxin-3 is associated with p53 mediated apoptosis [105, 106]. In addition, p53 was thought to share a common signaling pathway with oncogenesis [107]. That is to say,

p53 regulates the balance between survival and apoptosis. Still, more investigations on the possible role of p53 in MJD is required.

Collectively, our results revealed several important findings on glucose metabolism of Machado-Joseph disease. We showed that cells harboring full-length mutant ataxin-3 or truncated mutant ataxin-3 exhibited a significant decrease in glycolytic enzymes, including GLUT3 and PFK1. Moreover, knockdown CA8 caused a significant reduction in PFK1, indicating PFK1 is regulated by mutant ataxin-3 and CA8. In addition, given the fact that decreased expression of GLUT3 was observed in HEK293 cells expressing wild-type ataxin-3, significant increase of GLUT3 in cells expressing mutant ataxin-3 and truncated ataxin-3 may indicate a possible complementary effect for glucose uptake in the MJD model (Fig. S7). Nonetheless, overexpression of CA8 significantly increased the expression of GLUT3 and PFK1 in HEK293-MJD78 cells. Furthermore, we showed a protein-protein interaction between GLUT3 and CA8 by using cerebellar lysates from both 52 week-old wild-type and MJD transgenic mice. A co-localization of ataxin-3 and CA8 was also detected in HEK293 MJD cellular models. All these findings suggest that glucose

metabolism is impaired in Machado-Joseph disease, and the downstream molecules may be affected by the expression of CA8. When it comes to the regulation of glycolytic pathway, the expression of PFKFB3 and TIGAR showed a complementary effect to compensate the decreased GLUT3 and PFK1 in HEK293 cells with mutant ataxin-3. The influence of different CA8 expression on PFKFB3, p53 and TIGAR exhibited the diverse roles of CA8 under the effects of wild-type ataxin-3, full-length and truncated mutant ataxin-3 (table 1). The results further demonstrated that CA8 is not only involved in glycolytic pathway but also affects the regulation and balance of glycolysis in MJD cellular models. Although more experiments should be conducted to understand the detailed changes of glycolytic activity in this model, the current study is the first report illustrating the metabolic role of CA8 in Machado-Joseph Disease.

5. Reference

1. Jouanne, M., S. Rault, and A.S. Voisin-Chiret, *Tau protein aggregation in Alzheimer's disease: An attractive target for the development of novel therapeutic agents.* Eur J Med Chem, 2017. **139**: p. 153-167.
2. Schulz-Schaeffer, W.J., *The synaptic pathology of alpha-synuclein aggregation in dementia with Lewy bodies, Parkinson's disease and Parkinson's disease dementia.* Acta Neuropathol, 2010. **120**(2): p. 131-43.
3. Seidel, K., et al., *Polyglutamine aggregation in Huntington's disease and spinocerebellar ataxia type 3: similar mechanisms in aggregate formation.* Neuropathol Appl Neurobiol, 2016. **42**(2): p. 153-66.
4. Gales, L., et al., *Towards a structural understanding of the fibrillization pathway in Machado-Joseph's disease: trapping early oligomers of non-expanded ataxin-3.* J Mol Biol, 2005. **353**(3): p. 642-54.
5. Adegbuyiro, A., et al., *Proteins Containing Expanded Polyglutamine Tracts and Neurodegenerative Disease.* Biochemistry, 2017. **56**(9): p. 1199-1217.
6. Jimenez-Sanchez, M., et al., *Autophagy and polyglutamine diseases.* Prog Neurobiol, 2012. **97**(2): p. 67-82.
7. Kawaguchi, Y., et al., *CAG expansion in a novel gene fo Machado-Joseph disease at chromosome 14q32.1.* Nat Genetic, 1994. **8**: p. 221-228.
8. Paulson, H., *Machado-Joseph disease/spinocerebellar ataxia type 3.* Handb Clin Neurol, 2012. **103**: p. 437-49.
9. Durr, A., et al., *Spinocerebellar ataxia 3 and Machado-Joseph disease: clinical, molecular, and neuropathoIogicaI features.* American Neurological Association, 1996(39): p. 490-499.
10. Perez M. K., et al., *Recruitment and the Role of Nuclear Localization in Polyglutamine-mediated Aggregation.* The Journal of Cell Biology, 1998. **143**(6): p. 1457-1470.
11. Chai, Y., et al., *Live-cell imaging reveals divergent intracellular dynamics of polyglutamine disease proteins and supports a sequestration model of pathogenesis.* Proc Natl Acad Sci U S A, 2002. **99**(14): p. 9310-5.
12. Chai Y., et al., *Analysis of the role of heat shock protein (Hsp) molecular chaperones in polyglutamine disease.* The Journal of Neuroscience, 1999. **19**(23): p. 10338–10347.
13. Ellisdon, A.M., M.C. Pearce, and S.P. Bottomley, *Mechanisms of ataxin-3 misfolding and fibril formation: kinetic analysis of a disease-associated polyglutamine protein.* J Mol Biol, 2007. **368**(2): p. 595-605.
14. Haacke, A., et al., *Proteolytic cleavage of polyglutamine-expanded ataxin-3 is*

critical for aggregation and sequestration of non-expanded ataxin-3. Hum Mol Genet, 2006. **15**(4): p. 555-68.

15. Masino, L., et al., *The Josephin domain determines the morphological and mechanical properties of ataxin-3 fibrils.* Biophys J, 2011. **100**(8): p. 2033-42.
16. Berger, Z., et al., *Rapamycin alleviates toxicity of different aggregate-prone proteins.* Hum Mol Genet, 2006. **15**(3): p. 433-42.
17. Chou, A.H., et al., *Polyglutamine-expanded ataxin-3 causes cerebellar dysfunction of SCA3 transgenic mice by inducing transcriptional dysregulation.* Neurobiol Dis, 2008. **31**(1): p. 89-101.
18. Onofre, I., et al., *Fibroblasts of Machado Joseph Disease patients reveal autophagy impairment.* Sci Rep, 2016. **6**: p. 28220.
19. Goti, D., et al., *A mutant ataxin-3 putative-cleavage fragment in brains of Machado-Joseph disease patients and transgenic mice is cytotoxic above a critical concentration.* J Neurosci, 2004. **24**(45): p. 10266-79.
20. Ikeda, H., et al., *Expanded polyglutamine in the Machado-Joseph disease protein induces cell death in vitro and in vivo.* Nat Genet, 1996(13): p. 196-202.
21. Paulson, H., et al., *Intranucleari nclusion of expanded polyglutamine protein in spinicerebellar ataxia type 3.* Neuron, 1997(19): p. 333-344.
22. Wellington C. L., et al., *Caspase cleavage of gene products associated with triplet expansion disorders generates truncated fragments containing the polyglutamine tract.* J Biol Chem, 1998. **273**(15): p. 9158–9167.
23. Huen, N.Y. and H.Y. Chan, *Dynamic regulation of molecular chaperone gene expression in polyglutamine disease.* Biochem Biophys Res Commun, 2005. **334**(4): p. 1074-84.
24. Chang, W.H., et al., *Decreased protein synthesis of Hsp27 associated with cellular toxicity in a cell model of Machado-Joseph disease.* Neurosci Lett, 2009. **454**(2): p. 152-6.
25. Haacke, A., F.U. Hartl, and P. Breuer, *Calpain inhibition is sufficient to suppress aggregation of polyglutamine-expanded ataxin-3.* J Biol Chem, 2007. **282**(26): p. 18851-6.
26. Colomer Gould, V.F., et al., *A mutant ataxin-3 fragment results from processing at a site N-terminal to amino acid 190 in brain of Machado-Joseph disease-like transgenic mice.* Neurobiol Dis, 2007. **27**(3): p. 362-9.
27. Antony, P.M., et al., *Identification and functional dissection of localization signals within ataxin-3.* Neurobiol Dis, 2009. **36**(2): p. 280-92.
28. Breuer, P., et al., *Nuclear aggregation of polyglutamine-expanded ataxin-3: fragments escape the cytoplasmic quality control.* J Biol Chem, 2010. **285**(9): p. 6532-7.

29. Schmitt I., et al., *Characterization of the rat spinocerebellar ataxia type 3 gene.* Neurogenetics, 1997(1): p. 103-112.
30. Hamilton, J.M., *Rate and correlates of weight change in Huntington's disease.* Journal of Neurology, Neurosurgery & Psychiatry, 2004. **75**(2): p. 209-212.
31. Sanberg P., Fibiger H., and M. R., *Body weight and dietary factors in Huntington's disease patients compared with matched controls.* Med. J. Aust., 1981(1): p. 407-409.
32. Cemal K. Cemal, et al., *YAC transgenic mice carrying pathological alleles of the MJD1 locus exhibit a mild and slowly progressive cerebellar defici.* Hum Mol Genet, 2002. **11**(9): p. 1075-94.
33. Saute, J.A., et al., *Body mass index is inversely correlated with the expanded CAG repeat length in SCA3/MJD patients.* Cerebellum, 2012. **11**(3): p. 771-4.
34. Sjoblom, B., et al., *Two point mutations convert a catalytically inactive carbonic anhydrase-related (CARP) to an active enzyme.* FEBS Letters, 1996(398): p. 322-325.
35. Picaud, S.S., et al., *Crystal structure of human carbonic anhydrase-related protein VIII reveals the basis for catalytic silencing.* Proteins, 2009. **76**(2): p. 507-11.
36. Hirota, J., et al., *Carbonic anhydrase-related protein is a novel binding protein for inositol 1,4,5-trisphosphate receptor type 1.* Biochem J, 2003(372): p. 435-441.
37. Aspatwar, A., et al., *Carbonic anhydrase related protein VIII and its role in neurodegeneration and cancer.* Current Pharmaceutical Design, 2010. **16**(29): p. 3264-76.
38. Aspatwar, A., M.E.E. Tolvanen, and S. Parkkila, *Phylogeny and expression of carbonic anhydrase-related proteins.* BMC molecular biology, 2010. **11**(25).
39. Jiao, Y., et al., *Carbonic anhydrase-related protein VIII deficiency is associated with a distinctive lifelong gait disorder in waddles mice.* Genetics, 2005. **171**(3): p. 1239-46.
40. Turkmen, S., et al., *CA8 mutations cause a novel syndrome characterized by ataxia and mild mental retardation with predisposition to quadrupedal gait.* PLoS Genet, 2009. **5**(5): p. e1000487.
41. Kaya, N., et al., *Phenotypical spectrum of cerebellar ataxia associated with a novel mutation in the CA8 gene, encoding carbonic anhydrase (CA) VIII.* Am J Med Genet B Neuropsychiatr Genet, 2011. **156B**(7): p. 826-34.
42. Wang, T.K., et al., *Effects of carbonic anhydrase-related protein VIII on human cells harbouring an A8344G mitochondrial DNA mutation.* Biochem J, 2014. **459**(1): p. 149-60.

43. Bezprozvanny, I., *Calcium signaling and neurodegenerative diseases.* Trends Mol Med, 2009. **15**(3): p. 89-100.
44. Chen, X., et al., *Deranged calcium signaling and neurodegeneration in spinocerebellar ataxia type 3.* J Neurosci, 2008. **28**(48): p. 12713-24.
45. Nishikata, M., et al., *Carbonic Anhydrase-Related Protein VIII Promotes Colon Cancer Cell Growth.* Mol Carcinog, 2007. **46**(3): p. 208-14.
46. Ishihara, T., et al., *Carbonic anhydrase-related protein VIII increases invasiveness of non-small cell lung adenocarcinoma.* Virchows Arch, 2006. **448**(6): p. 830-7.
47. Warburg, O., *On the Origin of Cancer Cells.* Science, 1956. **123**(3191): p. 309-314.
48. Mulukutla, B.C., et al., *Multiplicity of steady states in glycolysis and shift of metabolic state in cultured mammalian cells.* PLoS One, 2015. **10**(3): p. e0121561.
49. Pelicano, H., et al., *Glycolysis inhibition for anticancer treatment.* Oncogene, 2006. **25**(34): p. 4633-46.
50. Hamanaka, R.B. and N.S. Chandel, *Targeting glucose metabolism for cancer therapy.* J Exp Med, 2012. **209**(2): p. 211-5.
51. TK.. Wang, et al., *Oncogenic roles of carbonic anhydrase 8 in human osteosarcoma cells.* Tumor Biol, 2015. **37**(6): p. 7989–8005.
52. Huang, M.S., et al., *Roles of carbonic anhydrase 8 in neuronal cells and zebrafish.* Biochim Biophys Acta, 2014. **1840**(9): p. 2829-42.
53. Cepeda-Prado, E., et al., *R6/2 Huntington's disease mice develop early and progressive abnormal brain metabolism and seizures.* J Neurosci, 2012. **32**(19): p. 6456-67.
54. Rodriguez-Quiroga, S.A., et al., *Huntington's disease masquerading as spinocerebellar ataxia.* BMJ Case Rep, 2013. **2013**.
55. Gamberino, W.C. and Brennan, W.A., *Glucose transporter isoform expression in Huntington's disease brain.* J. Neurochem, 1994. **63**(4): p. 1392-1397.
56. McClory, H., et al., *Glucose transporter 3 is a rab11-dependent trafficking cargo and its transport to the cell surface is reduced in neurons of CAG140 Huntington's disease mice.* Acta Neuropathol Commun, 2014. **2**: p. 179.
57. ED, B., G. JS, and S. EG, *Huntington's Chorea: Post Mortem Activity of Enzymes Involved in Cerebral Glucose Metabolsim.* J of Neurochem, 1977. **29**(3): p. 539-545.
58. Hsieh, M., et al., *Altered expression of carbonic anhydrase-related protein XI in neuronal cells expressing mutant ataxin-3.* Cerebellum, 2013. **12**(3): p. 338-49.
59. Wen, F.-C., et al., *Down-regulation of heat shock protein 27 in neuronal cells*

and non-neuronal cells expressing mutant ataxin-3. FEBS Letters, 2003. **546**(2-3): p. 307-314.

60. Lundgaard, I., et al., *Direct neuronal glucose uptake heralds activity-dependent increases in cerebral metabolism.* Nat Commun, 2015. **6**: p. 6807.
61. Leenders KL, et al., *Brain energy metabolism and dopaminergic function in Huntington's disease measured in vivo using positron emission tomography.* Mov. Disord, 1986. **1**(1): p. 69-77.
62. Mähler A, et al., *Increased catabolic state in spinocerebellar ataxia type 1 patients.* Cerebellum, 2014. **13**(4): p. 440-6.
63. Cemal K. Cemal, C.J.C., Lorraine Lawrence, Margaret B. Lowrie, Piers Ruddle, Sahar Al-Mahdawi, Rosalind H. M. King, Mark A. Pook, Clare Huxley and and S. Chamberlain, *YAC Transgenic Mice Carrying Pathological Alleles of the MJD1 Locus Exhibit a Mild and Slowly Progressive Cerebellar Defici.* Human Molecular Genetics, 2002: p. 11, 1075–1094.
64. Oh, M., et al., *Different subregional metabolism patterns in patients with cerebellar ataxia by 18F-fluorodeoxyglucose positron emission tomography.* PLoS One, 2017. **12**(3): p. e0173275.
65. Qin, W., et al., *Neuronal SIRT1 activation as a novel mechanism underlying the prevention of Alzheimer disease amyloid neuropathology by calorie restriction.* J Biol Chem, 2006. **281**(31): p. 21745-54.
66. Mather F, et al., *Expression of two glucose transporters, GLUT1 and GLUT3, in cultured cerebellar neurons: evidence for neuron-specific expression of GLUT3.* MOL CELL NEUROSCI, 1991. **2**: p. 351-360.
67. Wilson, J.E., *Isozymes of mammalian hexokinase: structure, subcellular localization and metabolic function.* Journal of Experimental Biology, 2003. **206**(12): p. 2049-2057.
68. Gimenez-Cassina, A., et al., *Mitochondrial hexokinase II promotes neuronal survival and acts downstream of glycogen synthase kinase-3.* J Biol Chem, 2009. **284**(5): p. 3001-11.
69. Weber, G., *Enzymology of cancer cells (second of two parts). New Engl J Med*, 1977(296): p. 541-551.
70. Hers, H. and E. Van Schaftingen, *Fructose 2,6-bisphosphate 2 years after its discovery.* J Biol Chem, 1982(206): p. 1-12.
71. Li, H., et al., *A role for inducible 6-phosphofructo-2-kinase in the control of neuronal glycolysis.* J Nutr Biochem, 2013. **24**(6): p. 1153-8.
72. Mather, F., et al., *Expression of Two Glucose Transporters, GLUT1 and GLUT3, in Cultured Cerebellar Neurons: Evidence for Neuron-Specific Expression of GLUT3.* MOL CELL NEUROSCI, 1991. **2**(4): p. 351-360.

73. Barros, L.F., et al., *Evidence of two mechanisms for the activation of the glucose transporter GLUT1 by a:nisomycin: p38 (MAP kinase) activation and protein synthesis inhibition in mammalian cells.* J. Physiol., 1997. **504**(3): p. 517-525.
74. Mueckler, M., *Family of Glucose-Transporter Genes: Implications for Glucose Homeostasis and Diabetes.* Diabetes, 1990. **39**: p. 6-11.
75. Vittori, A., et al., *Copy-number variation of the neuronal glucose transporter gene SLC2A3 and age of onset in Huntington's disease.* Hum Mol Genet, 2014. **23**(12): p. 3129-37.
76. Corona, J.C., et al., *Hexokinase II gene transfer protects against neurodegeneration in the rotenone and MPTP mouse models of Parkinson's disease.* J Neurosci Res, 2010. **88**(9): p. 1943-50.
77. Rose, I.A. and J.V.B. Warms, *Mitochondrial hexokinase: release, rebinding and location.* J Biol Chem, 1967. **424**(7): p. 1635-1645.
78. Davey, G.P., S. Peuchen, and J.B. Clark, *Energy thresholds in brain mitochondria: potential involvement in neurodegeneration.* J Biol Chem, 1998. **273**(21): p. 12753-12757.
79. Jenkins, C.M., et al., *Reversible high affinity inhibition of phosphofructokinase-1 by acyl-CoA: a mechanism integrating glycolytic flux with lipid metabolism.* J Biol Chem, 2011. **286**(14): p. 11937-50.
80. Yalcin, A., et al., *Regulation of glucose metabolism by 6-phosphofructo-2-kinase/fructose-2,6-bisphosphatases in cancer.* Exp Mol Pathol, 2009. **86**(3): p. 174-9.
81. Besson, M.T., et al., *Enhanced neuronal glucose transporter expression reveals metabolic choice in a HD Drosophila model.* PLoS One, 2015. **10**(3): p. e0118765.
82. Zhang, F., et al., *Phosphofructokinase-1 Negatively Regulates Neurogenesis from Neural Stem Cells.* Neurosci Bull, 2016. **32**(3): p. 205-16.
83. Jang, S., et al., *Glycolytic Enzymes Localize to Synapses under Energy Stress to Support Synaptic Function.* Neuron, 2016. **90**(2): p. 278-91.
84. Cura, A.J. and A. Carruthers, *Role of monosaccharide transport proteins in carbohydrate assimilation, distribution, metabolism, and homeostasis.* Compr Physiol, 2012. **2**(2): p. 863-914.
85. Shah, K., S. Desilva, and T. Abbruscato, *The role of glucose transporters in brain disease: diabetes and Alzheimer's Disease.* Int J Mol Sci, 2012. **13**(10): p. 12629-55.
86. Uemura, E. and H.W. Greenlee, *Insulin regulates neuronal glucose uptake by promoting translocation of glucose transporter GLUT3.* Exp Neurol, 2006. **198**(1): p. 48-53.
87. Hung, Y.P., et al., *Akt regulation of glycolysis mediates bioenergetic stability in*

epithelial cells. Elife, 2017. **6**.

88. Mor, I., E.C. Cheung, and K.H. Vousden, *Control of glycolysis through regulation of PFK1: old friends and recent additions.* Cold Spring Harb Symp Quant Biol, 2011. **76**: p. 211-6.
89. Yan, S., et al., *6-Phosphofructo-2-kinase/fructose-2,6-bisphosphatase isoform 3 spatially mediates autophagy through the AMPK signaling pathway.* Oncotarget, 2017. **8**(46): p. 80909-80922.
90. Sittler, A., et al., *Deregulation of autophagy in postmortem brains of Machado-Joseph disease patients.* Neuropathology, 2018. **38**(2): p. 113-124.
91. Gohil, V.M., et al., *Meclizine is neuroprotective in models of Huntington's disease.* Hum Mol Genet, 2011. **20**(2): p. 294-300.
92. Hong, C.T., K.Y. Chau, and A.H. Schapira, *Meclizine-induced enhanced glycolysis is neuroprotective in Parkinson disease cell models.* Sci Rep, 2016. **6**: p. 25344.
93. Okar, D., et al., *PFK-2/FBPase-2:maker and breaker of the essential biofactor fructose-2, 6-bisphosphate.* Trends Biochem Sci, 2001. **26**(1): p. 30-35.
94. Bensaad, K., et al., *TIGAR, a p53-inducible regulator of glycolysis and apoptosis.* Cell, 2006. **126**(1): p. 107-20.
95. Cao, L., et al., *Endogenous level of TIGAR in brain is associated with vulnerability of neurons to ischemic injury.* Neurosci Bull, 2015. **31**(5): p. 527-40.
96. Li, M., et al., *A TIGAR-regulated metabolic pathway is critical for protection of brain ischemia.* J Neurosci, 2014. **34**(22): p. 7458-71.
97. Singh, R., S. Sharad, and S. Kapur, *Free Radicals and Oxidative Stress in Neurodegenerative Diseases: Relevance of Dietary Antioxidants.* JIACM, 2004. **5**(3): p. 218-225.
98. Kumar, A. and R.R. Ratan, *Oxidative Stress and Huntington's Disease: The Good, The Bad, and The Ugly.* J Huntingtons Dis, 2016. **5**(3): p. 217-237.
99. Morrison, R.S. and Y. Kinoshita, *The role of p53 in neuronal cell death.* Cell Death Differ, 2000. **7**(10): p. 868-79.
100. Wang, D.B., et al., *p53 and mitochondrial function in neurons.* Biochim Biophys Acta, 2014. **1842**(8): p. 1186-97.
101. Chang, J.R., et al., *Role of p53 in neurodegenerative diseases.* Neurodegener Dis, 2012. **9**(2): p. 68-80.
102. Szybinska, A. and W. Lesniak, *P53 Dysfunction in Neurodegenerative Diseases - The Cause or Effect of Pathological Changes?* Aging Dis, 2017. **8**(4): p. 506-518.
103. Hock, A.K., et al., *Regulation of p53 stability and function by the deubiquitinating enzyme USP42.* EMBO J, 2011. **30**(24): p. 4921-30.
104. Liu, H., et al., *The Machado-Joseph Disease Deubiquitinase Ataxin-3 Regulates the Stability and Apoptotic Function of p53.* PLoS Biol, 2016. **14**(11): p.

e2000733.

105. Gao, R., et al., *Inactivation of PNKP by mutant ATXN3 triggers apoptosis by activating the DNA damage-response pathway in SCA3.* PLoS Genet, 2015. **11**(1): p. e1004834.

106. Chou, A.H., et al., *p53 activation mediates polyglutamine-expanded ataxin-3 upregulation of Bax expression in cerebellar and pontine nuclei neurons.* Neurochem Int, 2011. **58**(2): p. 145-52.

107. Lanni, C., et al., *p53 at the crossroads between cancer and neurodegeneration.* Free Radic Biol Med, 2012. **52**(9): p. 1727-33.

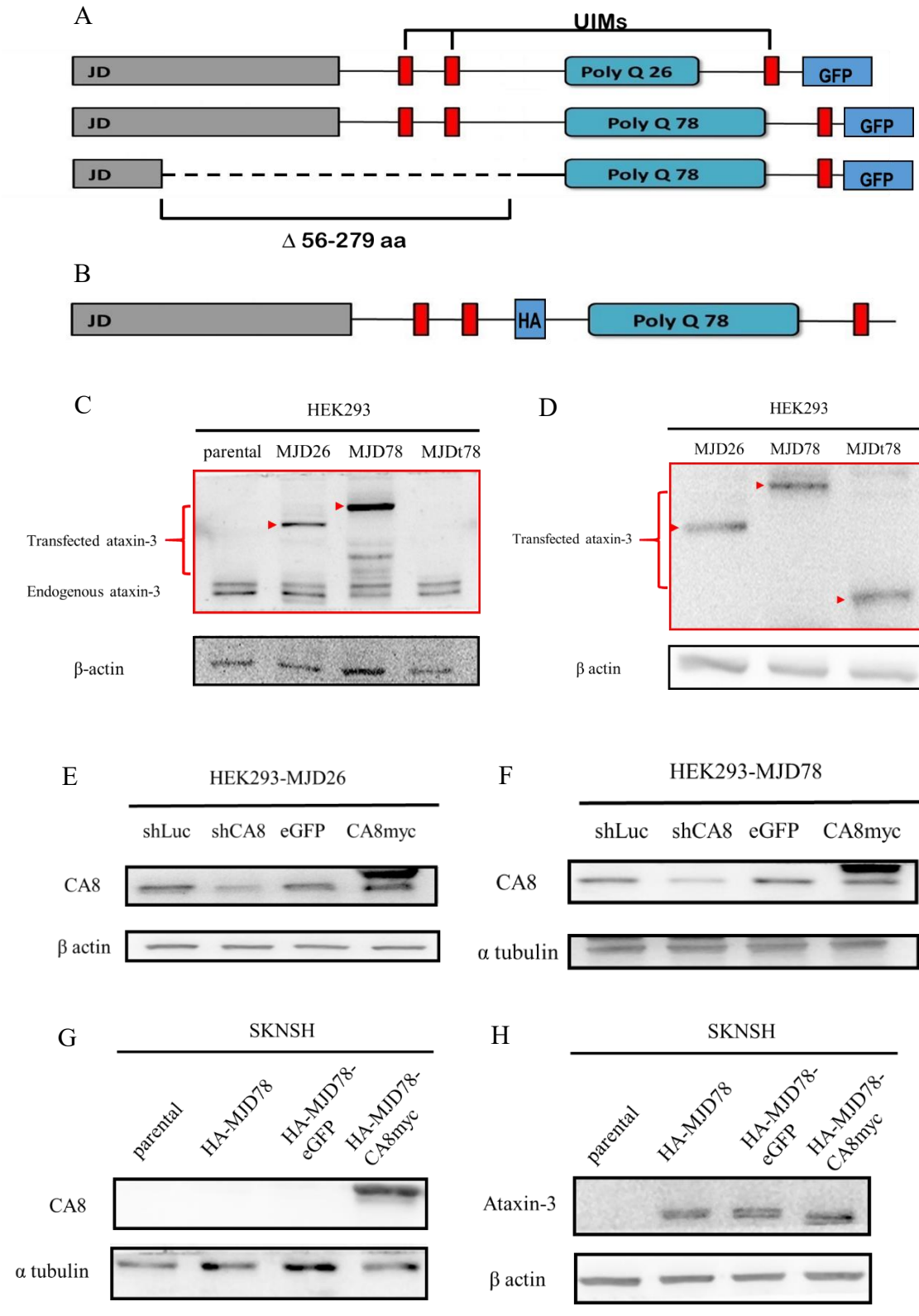
A
UIMs
JD
Poly Q 26
GFP
JD
Poly Q 78
GFP
JD
Poly Q 78
GFP
Δ 56-279 aa
B
JD
HA
Poly Q 78
C
HEK293
parental
MJD26
MJD78
MJDt78
Transfected ataxin-3
Endogenous ataxin-3
β-actin
D
HEK293
MJD26
MJD78
MJDt78
Transfected ataxin-3
β actin
E
HEK293-MJD26
shLuc
shCA8
eGFP
CA8myc
CA8
β actin
F
HEK293-MJD78
shLuc
shCA8
eGFP
CA8myc
CA8
α tubulin
G
SKNSH
parental
HA-MJD78
HA-MJD78-eGFP
HA-MJD78-CA8myc
CA8
α tubulin
H
SKNSH
parental
HA-MJD78
HA-MJD78-eGFP
HA-MJD78-CA8myc
Ataxin-3
β actin

Figure 1. Protein expression of CA8 and ataxin-3 in HEK293 cells. (A) A schematic diagram to illustrate three constructs containing ataxin-3 with 26 CAG repeats, 78 CAG repeats and N-terminal truncated 78 CAG repeats. Every constructs have a GFP fusion protein attached at N-terminus. UIMs are ubiquitin-interacting motifs. (B) A schematic diagram to illustrate the construct containing ataxin-3 with 78 CAG repeats, and a HA fusion protein attached at C-terminus (C) Protein expression of ataxin-3 in HEK293-MJD26, HEK293-MJD78 and HEK293-MJDt78. Endogenous ataxin-3 and mutant ataxin-3 were detected by antibody against ataxin-3. (D) Expression of ataxin-3 was detected by antibody against GFP in HEK293-MJD26, HEK293-MJD78 and HEK293-MJDt78. (E)(F) Western blot analysis of CA8 expression in HEK293-MJD26, HEK293-MJD78, respectively. Cells were infected with lentivirus to knockdown CA8 or overexpress CA8. shLuc was used as control of shCA8 and eGFP was used as control of CA8myc. (G) Expression of mutant ataxin-3 was detected in SK-N-SH-parental, SK-N-SH-HAMJD78, SK-N-SH-HAMJD78-eGFP and SK-N-SH-HAMJD78-CA8myc. Mutant ataxin-3 were detected by antibody against ataxin-3. (H) Western blot analysis of CA8 expression in SK-N-SH cells. The endogenous expression of CA8 was absence in SK-N-SH, the band represented CA8myc signal. ß actin and α tubulin were examined for loading control.

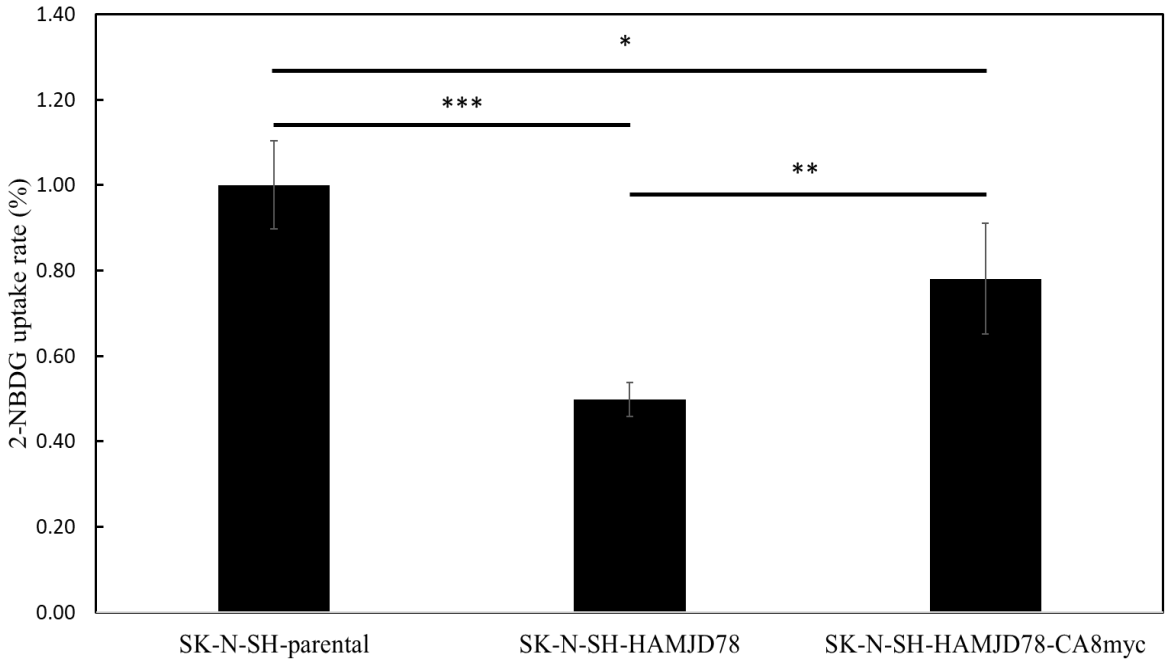

Figure. 2 The ability of glucose uptake is reduced in the presence of mutant ataxin-3. SK-N-SH-parental, SK-N-SH-HAMJD78 and SK-N-SH-HAMJD78-CA8myc cells were seeded at 1.3×10^5 cells/well. After 24 hr, cells were conducted to 2-NBDG uptake assay. The fluorescence value was recorded by SpectraMax M2e Microplate Readers. The 2-NBDG uptake rate of SK-N-SH cells expressing mutant ataxin-3 was significant lower than parental cells. Overexpression of CA8 in SK-N-SH cells harboring mutant ataxin-3 significantly increased 2-NBDG uptake rate. Data was expressed as means ± SEM from two four experiments. *$p<0.05$, **$p<0.01$, ***$p<0.001$

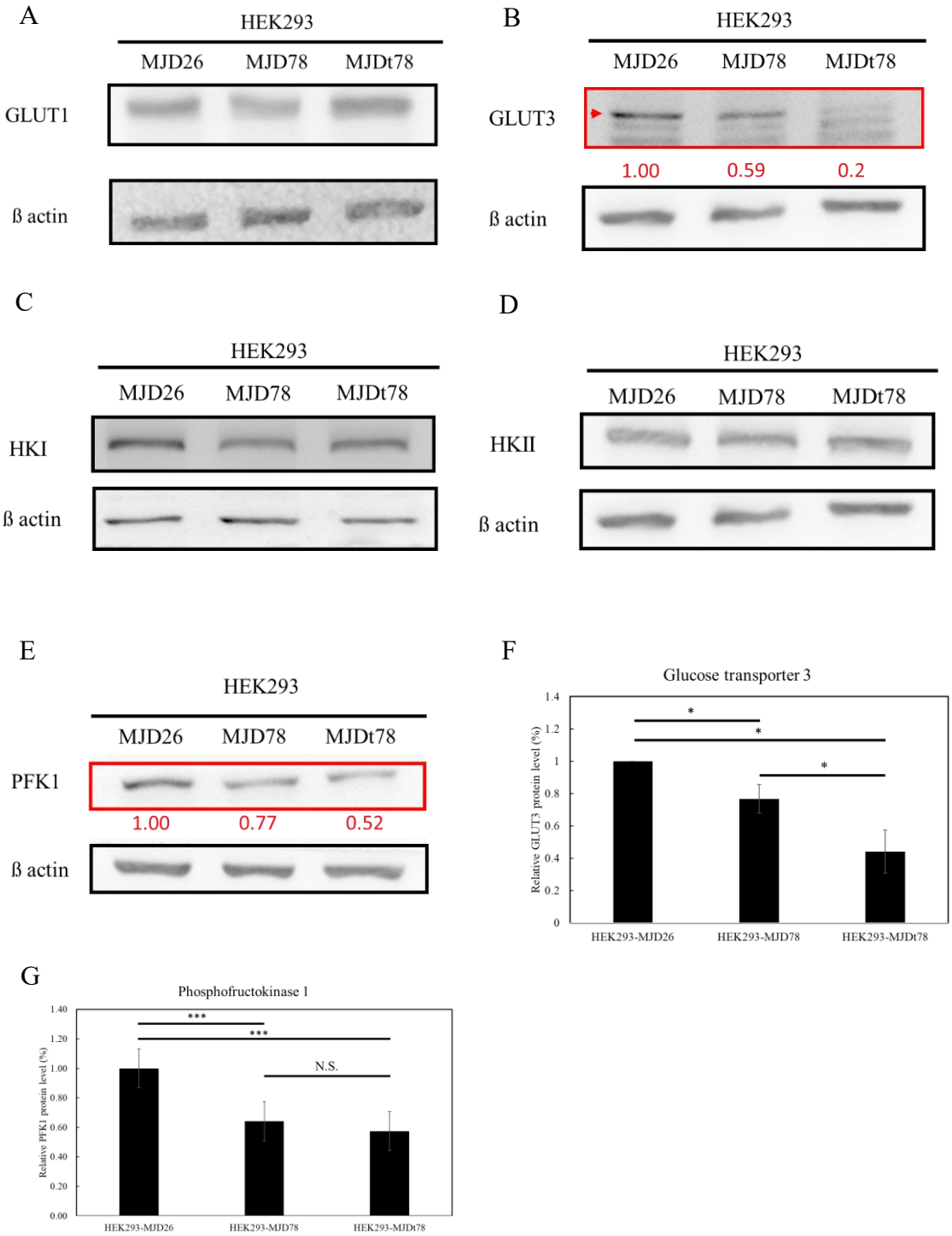
A
HEK293
MJD26
MJD78
MJDt78
GLUT1
ß actin
B
HEK293
MJD26
MJD78
MJDt78
GLUT3
1.00
0.59
0.2
ß actin
C
HEK293
MJD26
MJD78
MJDt78
HKI
ß actin
D
HEK293
MJD26
MJD78
MJDt78
HKII
ß actin
E
HEK293
MJD26
MJD78
MJDt78
PFK1
1.00
0.77
0.52
ß actin
F
Glucose transporter 3
Relative GLUT3 protein level (%)
HEK293-MJD26
HEK293-MJD78
HEK293-MJDt78
G
Phosphofructokinase 1
Relative PFK1 protein level (%)
N.S.
HEK293-MJD26
HEK293-MJD78
HEK293-MJDt78

Figure. 3 The expression of glycolytic enzymes is decreased in cells expressing mutant ataxin-3. (A) Western blot analysis of GLUT1 expression in HEK293 cell lines. (B) Expression of GLUT3. (C) Protein expression of HKI was detected in HEK293 cell lines. (D) HKII protein expression was examined in HEK293 cell lines. (E) PFK1 protein expression was analyzed in HEK293 cell lines. Results were evaluated by Western blot. Protein expression was probed with antibody against GLUT1, GLUT3, HKI, HKII, PFK1. ß actin was examined for loading control. (F)(G) Quantitative analysis of GLUT3 and PFK1 protein expression. Data was expressed as means ± SEM from at least three separate experiments. *$p<0.05$, **$p<0.01$, ***$p<0.001$, N.S.=non-significant

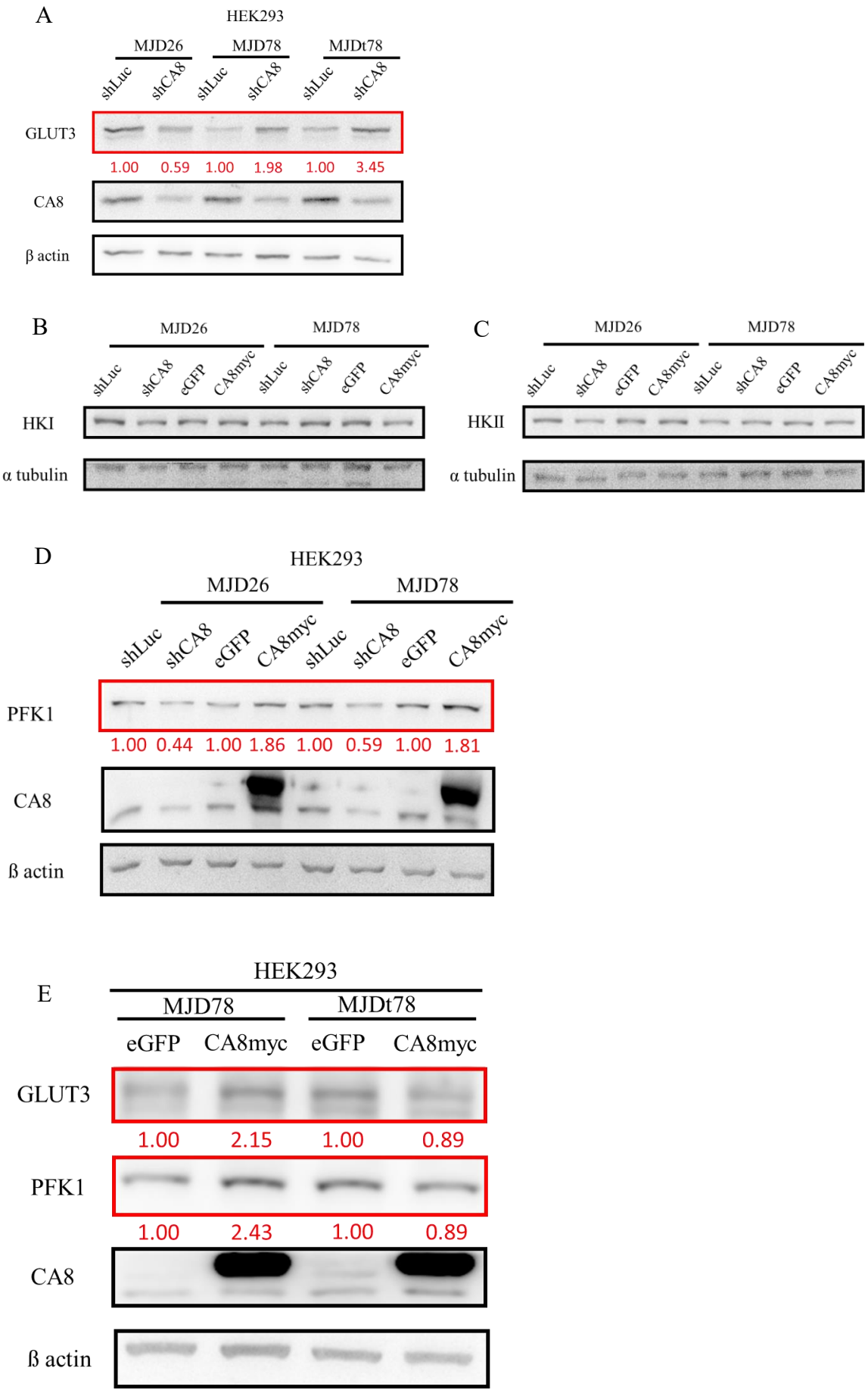
A
HEK293
MJD26
MJD78
MJDt78
shLuc
shCA8
shLuc
shCA8
shLuc
shCA8
GLUT3
1.00 0.59 1.00 1.98 1.00 3.45
CA8
β actin
B
MJD26
MJD78
shLuc
shCA8
eGFP
CA8myc
shLuc
shCA8
eGFP
CA8myc
HKI
α tubulin
C
MJD26
MJD78
shLuc
shCA8
eGFP
CA8myc
shLuc
shCA8
eGFP
CA8myc
HKII
α tubulin
D
HEK293
MJD26
MJD78
shLuc
shCA8
eGFP
CA8myc
shLuc
shCA8
eGFP
CA8myc
PFK1
1.00 0.44 1.00 1.86 1.00 0.59 1.00 1.81
CA8
ß actin
E
HEK293
MJD78
MJDt78
eGFP
CA8myc
eGFP
CA8myc
GLUT3
1.00 2.15 1.00 0.89
PFK1
1.00 2.43 1.00 0.89
CA8
ß actin

F

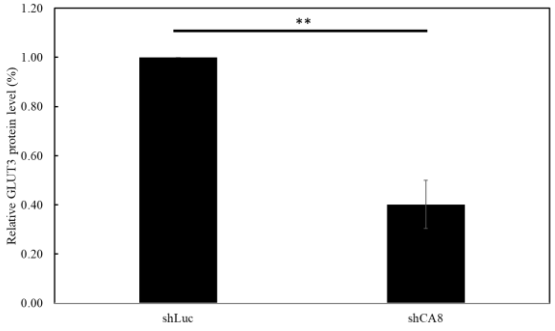
HEK293-MJD26
Relative GLUT3 protein level (%)
1.20
1.00
0.80
0.60
0.40
0.20
0.00
**
shLuc
shCA8

G

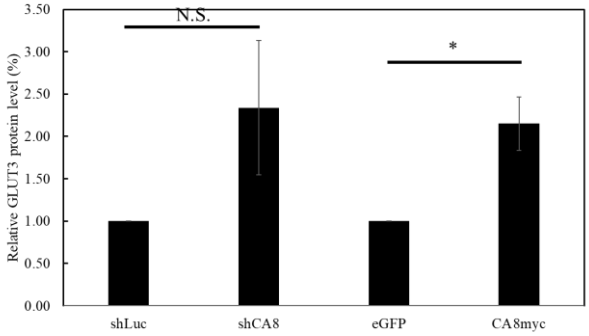
HEK293-MJD78
Relative GLUT3 protein level (%)
3.50
3.00
2.50
2.00
1.50
1.00
0.50
0.00
N.S.
*
shLuc
shCA8
eGFP
CA8myc

H

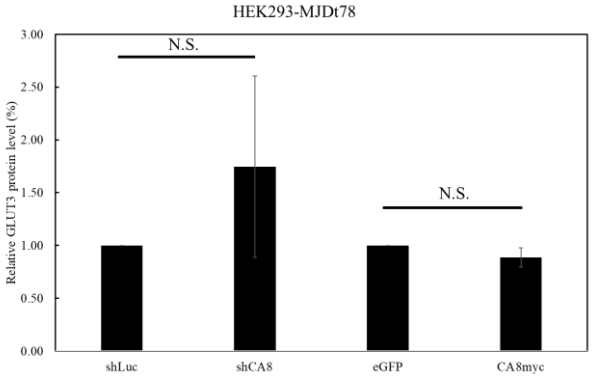
HEK293-MJDt78
Relative GLUT3 protein level (%)
3.00
2.50
2.00
1.50
1.00
0.50
0.00
N.S.
N.S.
shLuc
shCA8
eGFP
CA8myc

I

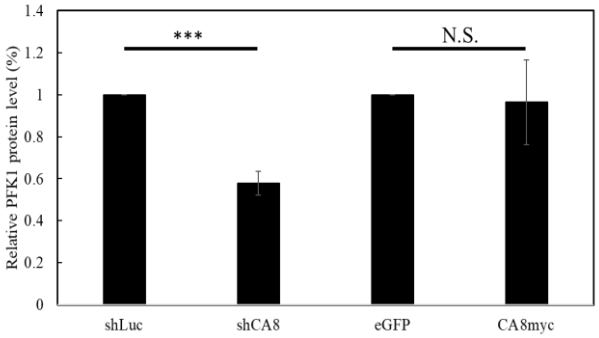
HEK293-MJD26
Relative PFK1 protein level (%)
1.4
1.2
1
0.8
0.6
0.4
0.2
0
***
N.S.
shLuc
shCA8
eGFP
CA8myc

J

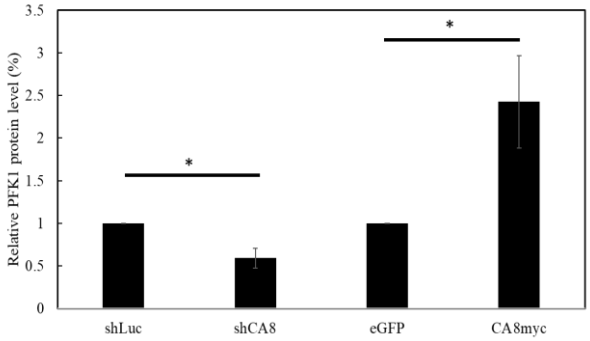
HEK293-MJD78
Relative PFK1 protein level (%)
3.5
3
2.5
2
1.5
1
0.5
0
*
*
shLuc
shCA8
eGFP
CA8myc

K

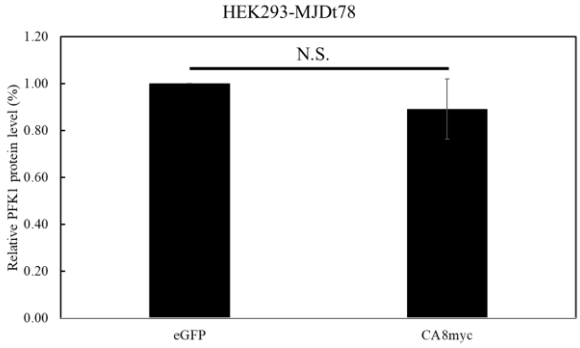
HEK293-MJDt78
Relative PFK1 protein level (%)
1.20
1.00
0.80
0.60
0.40
0.20
0.00
N.S.
eGFP
CA8myc

Figure. 4 Down-regulation of CA8 decreases expression of glycolytic enzymes

(A) Western blot analysis of GLUT3 in HEK293 MJD cellular models with CA8 down-regulation. (B)(C) HKI and HKII protein expression were examined by Western blot. (D) Protein expression of PFK1 in CA8 down-regulated HEK293-MJD26 and HEK293-MJD78 respectively. Antibodies against GLUT3, HKI, HKII, PFK1 were used. (E) Protein expression of GLUT3 and PFK1 were evaluated in HEK293-MJD78 and HEK293-MJDt78 with overexpressed CA8. ß actin and α tubulin were used for loading control. (F)(G)(H) Quantitative analysis of GLUT3 protein expression in HEK293-MJD26, HEK293-MJD78 and HEK293-MJDt78 with different CA8 expression. (I)(J)(K) Quantitative analysis of PFK1 protein expression in HEK293-MJD26, HEK293-MJD78 and HEK293-MJDt78 with different CA8 expression. Data was expressed as means ± SEM from at least three separate experiments. *$p<0.05$, **$p<0.01$. N.S.=non-significant.

A

52w-WT 40X

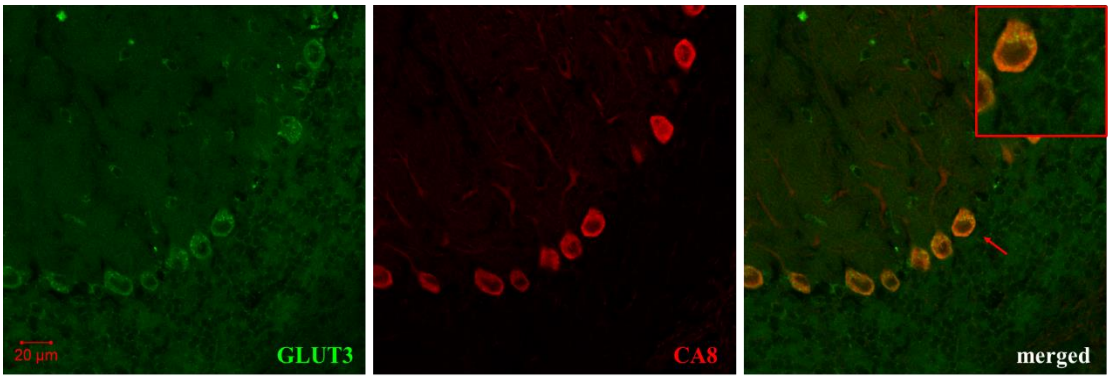

52w-SCA3 40X

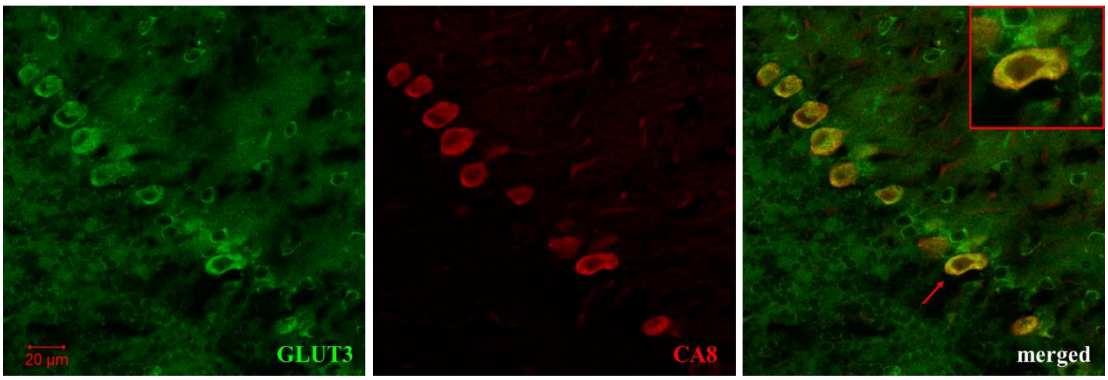

B

HEK293-MJD26
63X

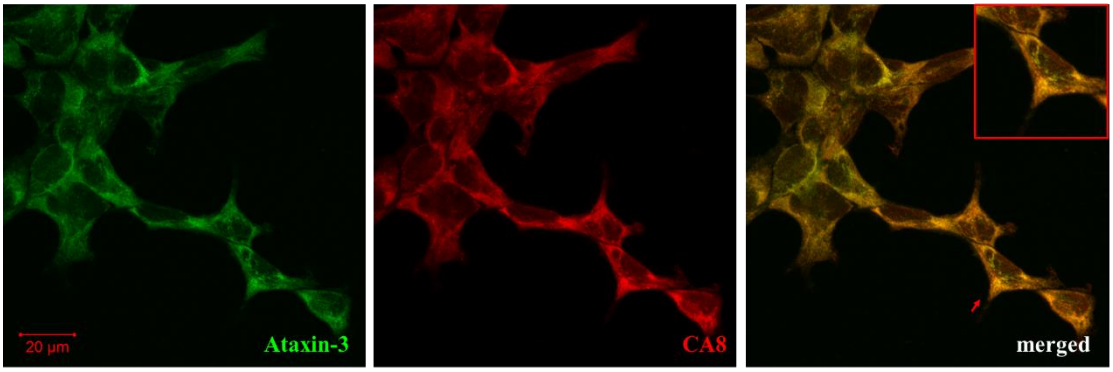

HEK293-MJD78
63X

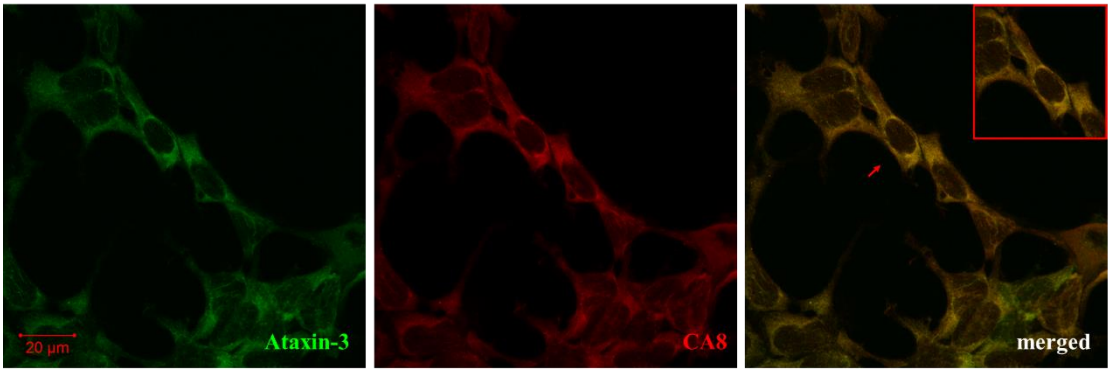

Figure. 6 CA8 is co-localized with GLUT3 both in MJD transgenic mice and HEK293 MJD cell models. (A) CA8 was partially co-localized with GLUT3 in cerebellum of 52 week-old wild-type mice (upper figure) and MJD transgenic mice (lower figure). Cerebellum tissue was analyzed by frozen section. Double staining indicated a partially co-localization (yellow) of CA8 (red) and GLUT3 (green). (B) CA8 was partially co-localized with ataxin-3 in HEK293-MJD26 and HEK293-MJD78. Double staining indicated a partially co-localization (yellow) of CA8 (red) and ataxin-3 (green). Immunofluorescence staining was conducted by antibody against CA8, GLUT3, ataxin-3.

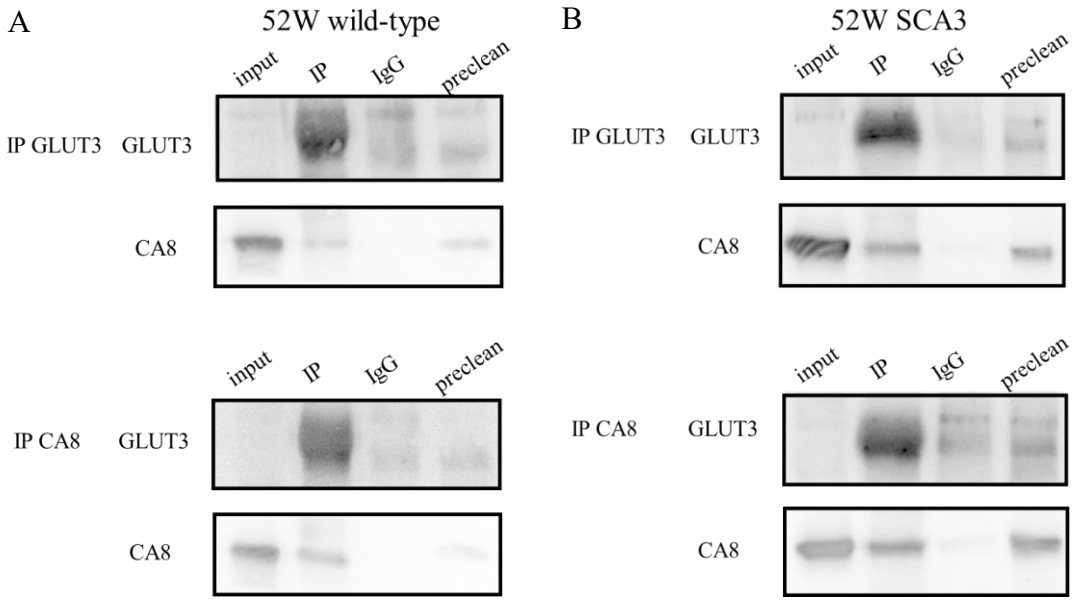

Figure. 5 CA8 interacts with GLUT3 both in wild-type and MJD transgenic mouse. (A) The protein lysates were harvested from cerebellum of 52 week-old wild-type mice. Proteins were precipitated by antibody against GLUT3 or CA8 respectively, and probed by Western blot with antibody against GLUT3 and CA8. (B) The protein lysates were harvested from cerebellum of 52 week-old MJD transgenic mice. Proteins were precipitated by antibody against GLUT3 or CA8 respectively, and probed by Western blot with antibody against GLUT3 and CA8. The input containing 30ug of protein lysates. IgG was used as a negative control in the experiment. Preclean was conducted by incubation of beads and protein lysates.

A

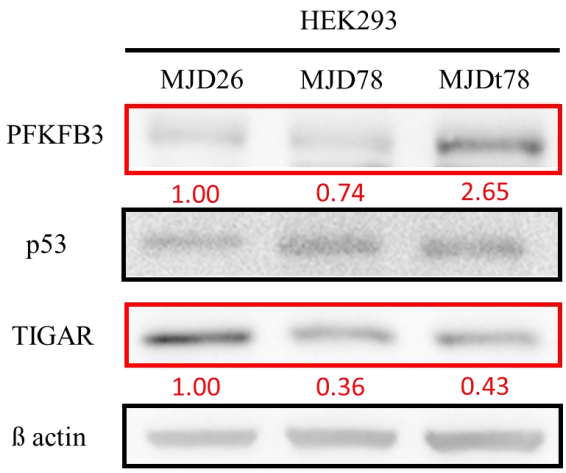
HEK293
MJD26
MJD78
MJDt78
PFKFB3
1.00
0.74
2.65
p53
TIGAR
1.00
0.36
0.43
ß actin

B

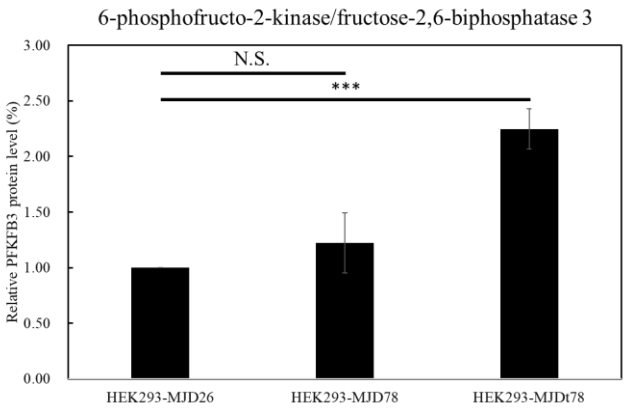
6-phosphofructo-2-kinase/fructose-2,6-biphosphatase 3
Relative PFKFB3 protein level (%)
3.00
2.50
2.00
1.50
1.00
0.50
0.00
N.S.
***
HEK293-MJD26
HEK293-MJD78
HEK293-MJDt78

C

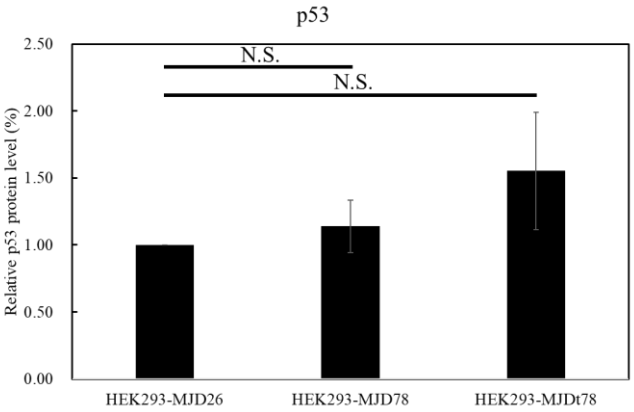
p53
Relative p53 protein level (%)
2.50
2.00
1.50
1.00
0.50
0.00
N.S.
N.S.
HEK293-MJD26
HEK293-MJD78
HEK293-MJDt78

D

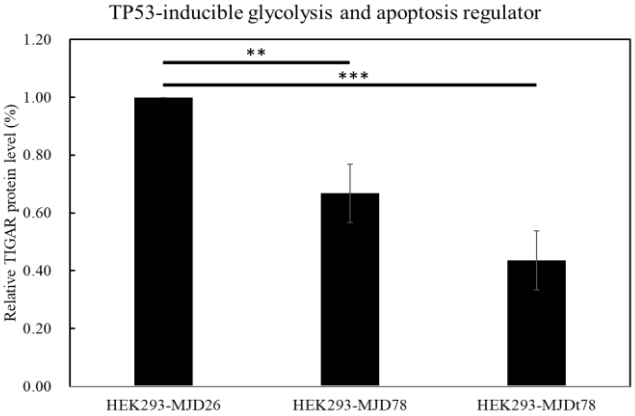
TP53-inducible glycolysis and apoptosis regulator
Relative TIGAR protein level (%)
1.20
1.00
0.80
0.60
0.40
0.20
0.00
**
***
HEK293-MJD26
HEK293-MJD78
HEK293-MJDt78

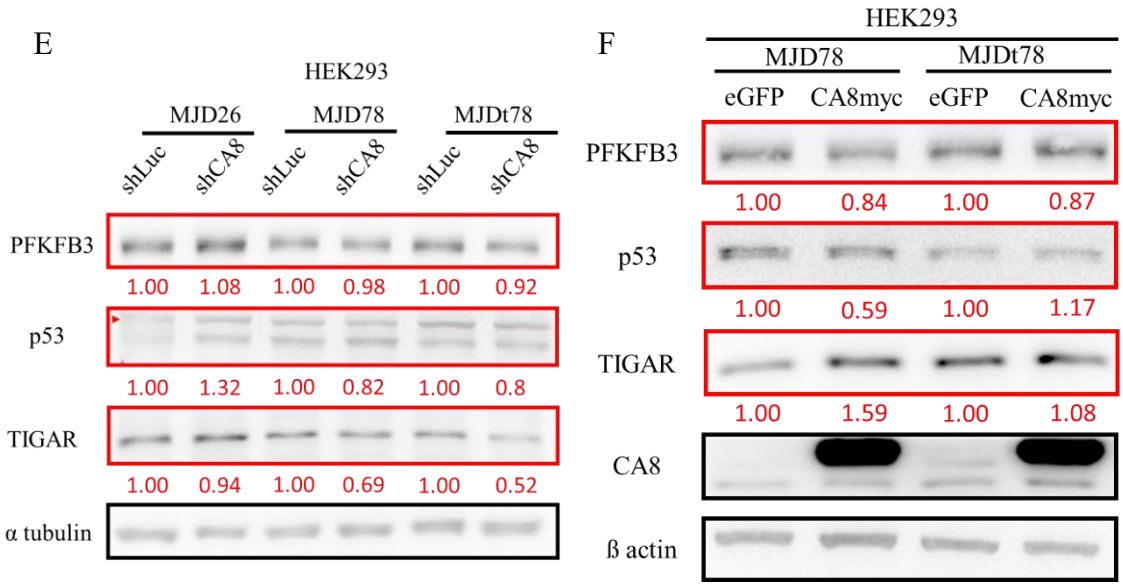
E
HEK293
MJD26
MJD78
MJDt78
shLuc
shCA8
shLuc
shCA8
shLuc
shCA8
PFKFB3
1.00 1.08 1.00 0.98 1.00 0.92
p53
1.00 1.32 1.00 0.82 1.00 0.8
TIGAR
1.00 0.94 1.00 0.69 1.00 0.52
α tubulin
F
HEK293
MJD78
MJDt78
eGFP
CA8myc
eGFP
CA8myc
PFKFB3
1.00 0.84 1.00 0.87
p53
1.00 0.59 1.00 1.17
TIGAR
1.00 1.59 1.00 1.08
CA8
ß actin

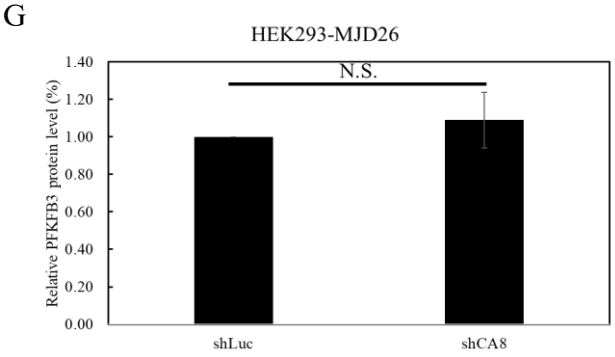
G
HEK293-MJD26
N.S.
Relative PFKFB3 protein level (%)
1.40
1.20
1.00
0.80
0.60
0.40
0.20
0.00
shLuc
shCA8

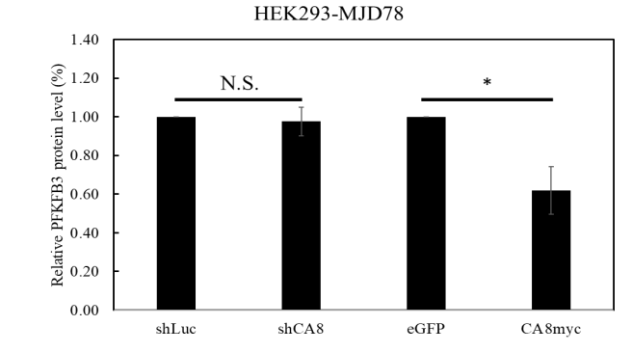
H
HEK293-MJD78
N.S.
*
Relative PFKFB3 protein level (%)
1.40
1.20
1.00
0.80
0.60
0.40
0.20
0.00
shLuc
shCA8
eGFP
CA8myc

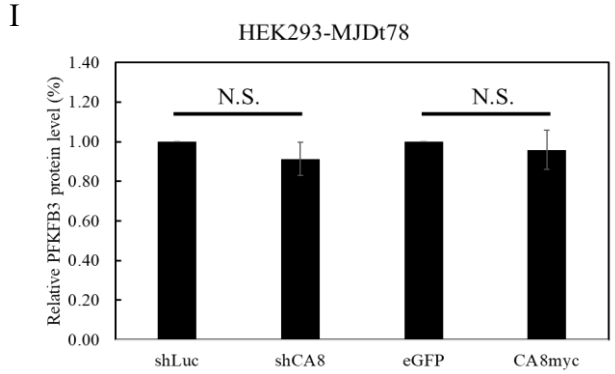
I
HEK293-MJDt78
N.S.
N.S.
Relative PFKFB3 protein level (%)
1.40
1.20
1.00
0.80
0.60
0.40
0.20
0.00
shLuc
shCA8
eGFP
CA8myc

J

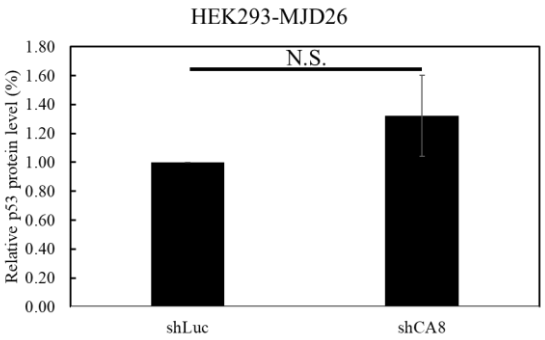
HEK293-MJD26
Relative p53 protein level (%)
1.80
1.60
1.40
1.20
1.00
0.80
0.60
0.40
0.20
0.00
N.S.
shLuc
shCA8

K

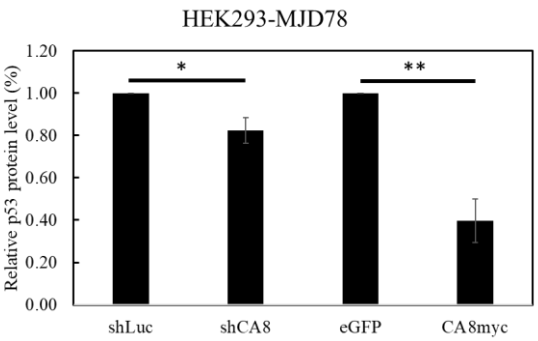
HEK293-MJD78
Relative p53 protein level (%)
1.20
1.00
0.80
0.60
0.40
0.20
0.00
*
**
shLuc
shCA8
eGFP
CA8myc

L

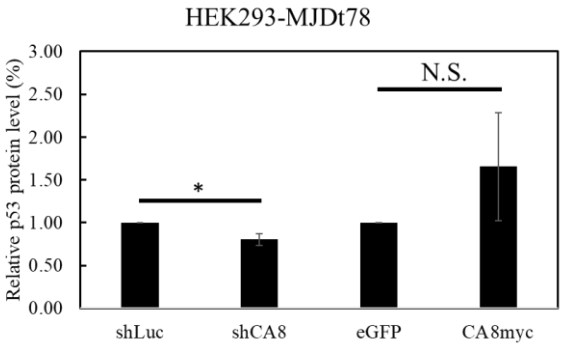
HEK293-MJDt78
Relative p53 protein level (%)
3.00
2.50
2.00
1.50
1.00
0.50
0.00
*
N.S.
shLuc
shCA8
eGFP
CA8myc

M

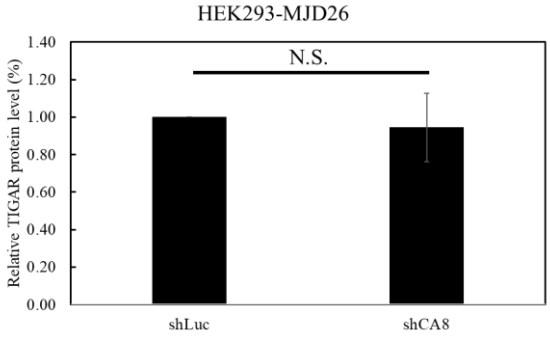
HEK293-MJD26
Relative TIGAR protein level (%)
1.40
1.20
1.00
0.80
0.60
0.40
0.20
0.00
N.S.
shLuc
shCA8

N

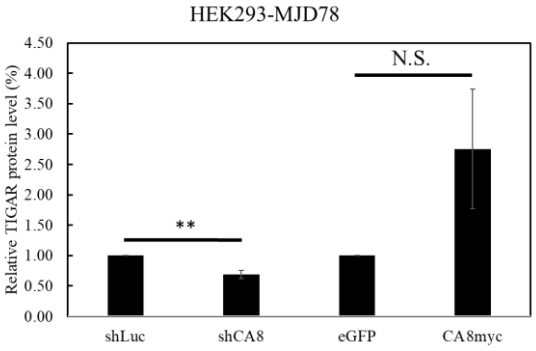
HEK293-MJD78
Relative TIGAR protein level (%)
4.50
4.00
3.50
3.00
2.50
2.00
1.50
1.00
0.50
0.00
**
N.S.
shLuc
shCA8
eGFP
CA8myc

O

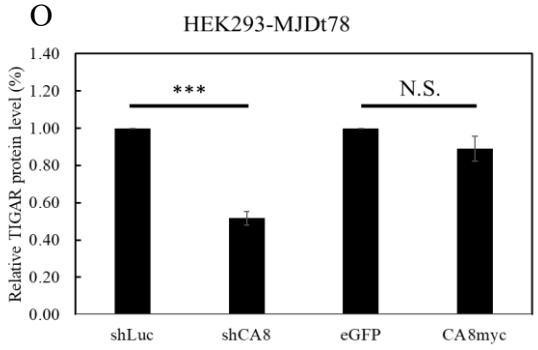
HEK293-MJDt78
Relative TIGAR protein level (%)
1.40
1.20
1.00
0.80
0.60
0.40
0.20
0.00
***
N.S.
shLuc
shCA8
eGFP
CA8myc

Figure. 7 The reduced glycolytic activity may be due to the decreased expression of TIGAR. (A)Western blot analysis of PFKFB3, p53, TIGAR in the presence of wild-type or mutant ataxin-3. (B) Quantitative analysis of PBKFB3 protein expression in HEK29 MJD cellular models. (C) Quantitative analysis of p53 protein expression in HEK29 MJD cellular models. (D) Quantitative analysis of TIGAR protein expression in HEK29 MJD cellular models. (E) Western blot analysis of PFKFB3, p53, TIGAR in HEK293-MJD26, HEK293-MJD78, HEK293-MJDt78 with down-regulated CA8. (F) Western blot analysis of PFKFB3, p53, TIGAR in HEK293-MJD26, HEK293-MJD78, HEK293-MJDt78 with overexpressed CA8. (G)(H)(I) Quantitative analysis of PFKFB3 protein expression in HEK293-MJD26, HEK293-MJD78 and HEK293-MJDt78 with different CA8 expression. (J)(K)(L) Quantitative analysis of p53 protein expression in HEK293-MJD26, HEK293-MJD78 and HEK293-MJDt78 with different CA8 expression. (M)(N)(O) Quantitative analysis of TIGAR protein expression in HEK293-MJD26, HEK293-MJD78 and HEK293-MJDt78 with different CA8 expression. Results were evaluated by Western blot. Protein expression was probed with antibody against PFKFB3, p53, TIGAR. ß actin and α tubulin was examined for internal control. Data was expressed as means ± SEM from at least three separate experiments. *$p<0.05$, **$p<0.01$, ***$p<0.001$, N.S.=non-significant.

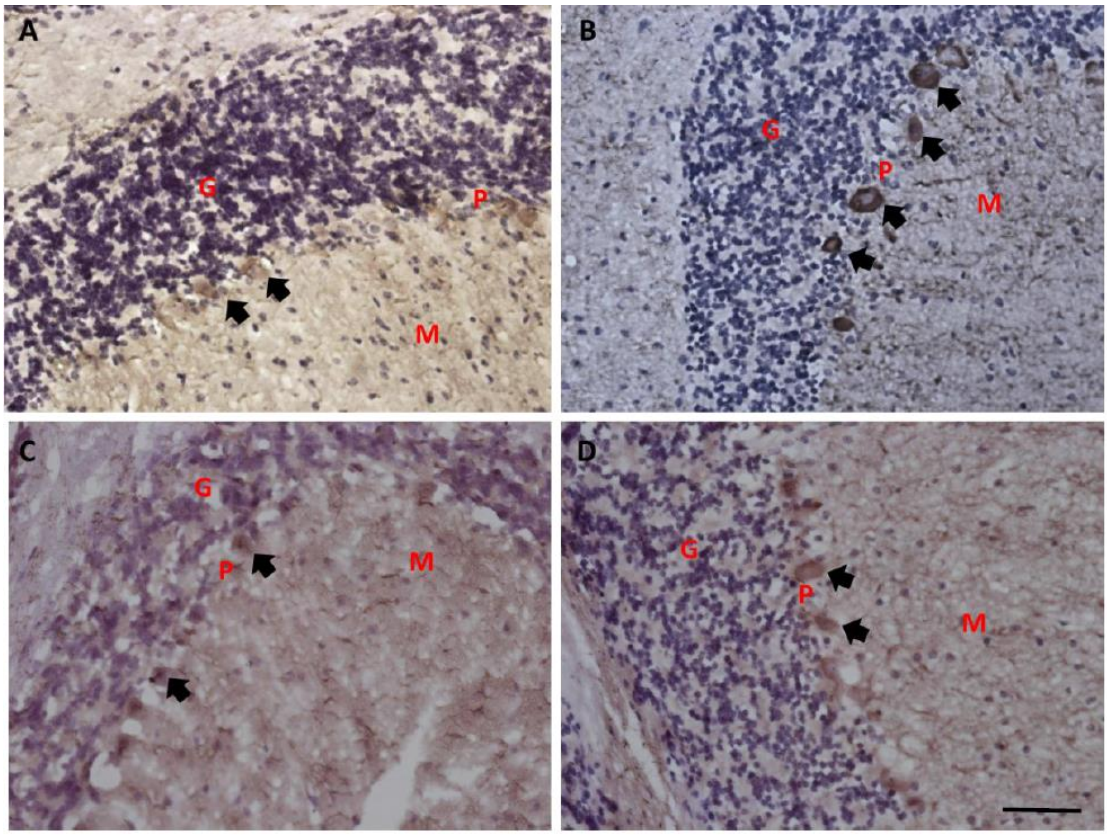
A
G
P
M
B
G
P
M
C
G
P
M
D
G
P
M

E

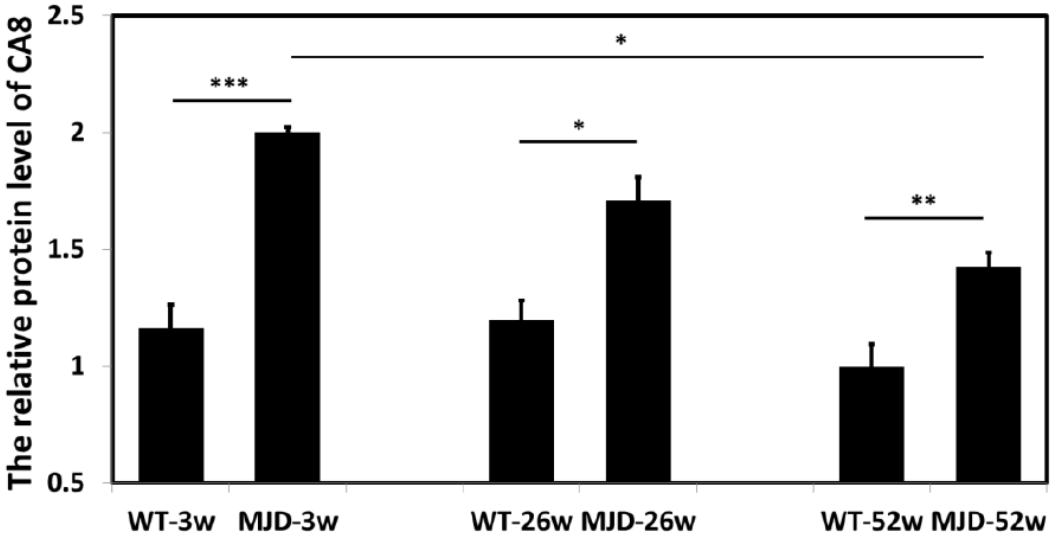
The relative protein level of CA8
2.5
2
1.5
1
0.5
***
*
*
**
WT-3w
MJD-3w
WT-26w
MJD-26w
WT-52w
MJD-52w

Figure. S1. Expression of CA8 was increased in the cerebellum of MJD transgenic mice. CA8 was detected in Purkinje cells by immunohistochemistry staining (arrow sign) (A)(C) Wild-type control of 3 week-old and 52 week-old mice respectively. (B)(D) The more intense staining was observed in 3 week-old and 52 week-old MJD transgenic mice. (E) The quantitative analysis indicated a significant increased CA8 expression in Purkinje cells of MJD transgenic mice of either 3 weesk or 52 weeks, as compared with their wild-type control. Data was expressed as Kruskal-Wallis test from six separate experiments. *$p<0.05$, **$p<0.01$, *** $p<0.001$.

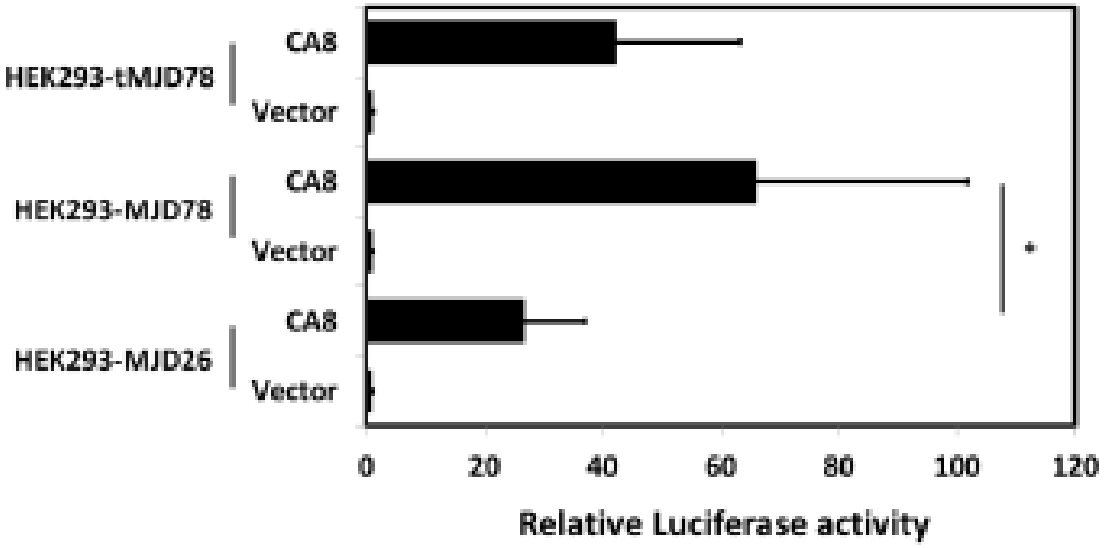

Figure. S2. Transcriptional activity of CA8 promoter was increased in HEK293 cells expressing mutant ataxin-3. A construct containing the full-length of CA8 promoter region cloned into luciferase vector was co-transfected into HEK293 MJD cell lines along with a β-gal vector. The luciferase activity of HEK293-MJD78 was higher than HEK293-MJD26. Relative luciferase was calculated with respect to cells transfected with vector alone. Data was expressed as means ± SEM from three separate experiments. *$p<0.05$.

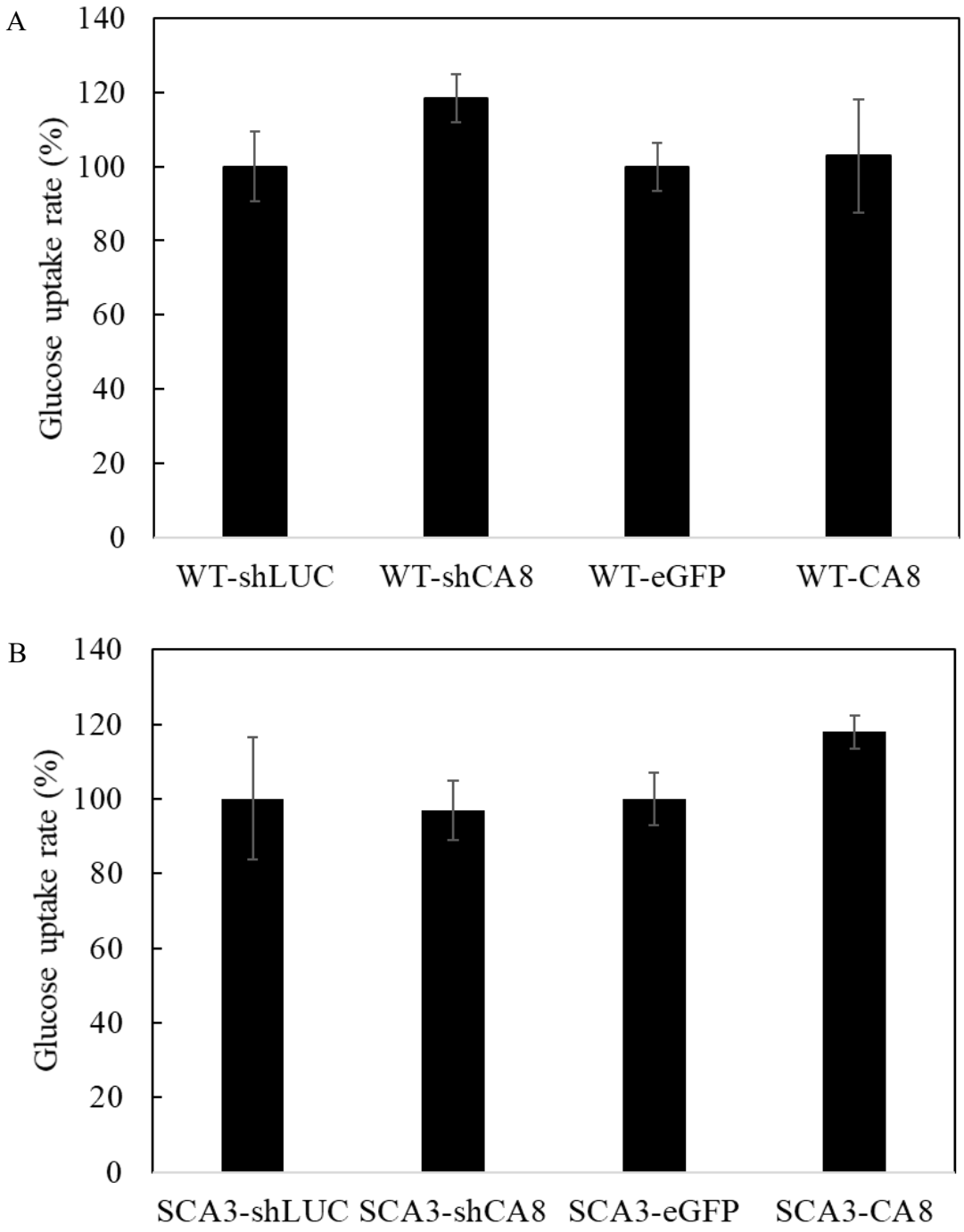

Figure. S3. CA8 overexpression partially rescued glucose uptake in cerebellar granule neurons of MJD transgenic mice. (A) In wild-type cerebellar granule neurons, there showed no significant difference with or without CA8 (B) Glucose uptake was partially increased in MJD cerebellar granule neurons.

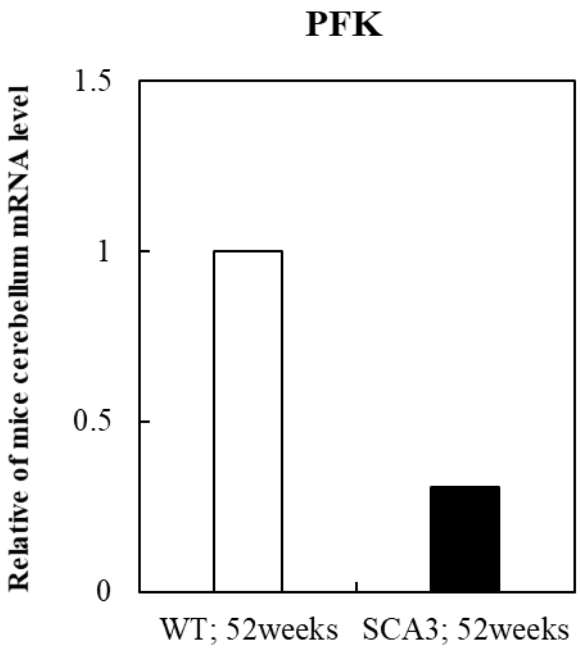

Figure. S4. A decreased PFK1 mRNA level in cerebellum of in 52 week-old MJD transgenic mice was observed. mRNA was extracted from cerebellar tissue of 52 week-old wild-type or MJD transgenic mice and analyzed by qPCR using PFK1 primer. Quantitative analysis was conducted by normalized to GAPDH mRNA levels.

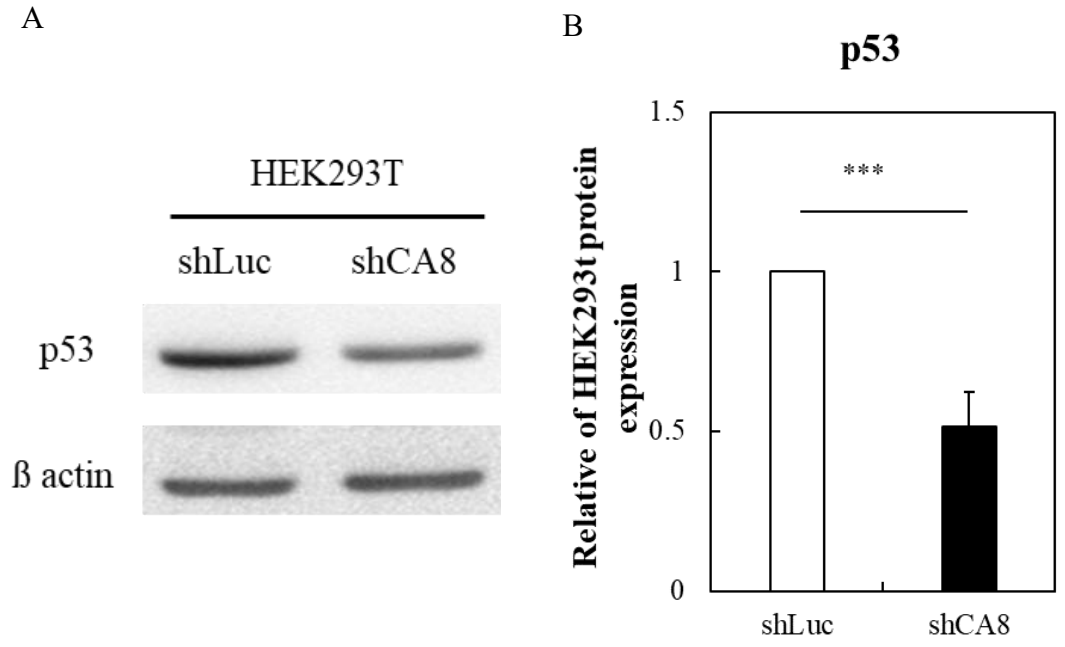

Figure. S5. Protein expression of p53 was significantly decreased in HEK293T cells with down-regulated CA8. (A) Western blot analysis of p53 protein expression in HEK293T cells with transiently down-regulated CA8. Antibodies against p53 was used. ß actin was examined for loading control. (B) Quantitative analysis of p53 protein expression in HEK293T-shLuc and HEK293T-shCA8. Data was expressed as means ± SEM from three separate experiments. ***$p<0.001$.

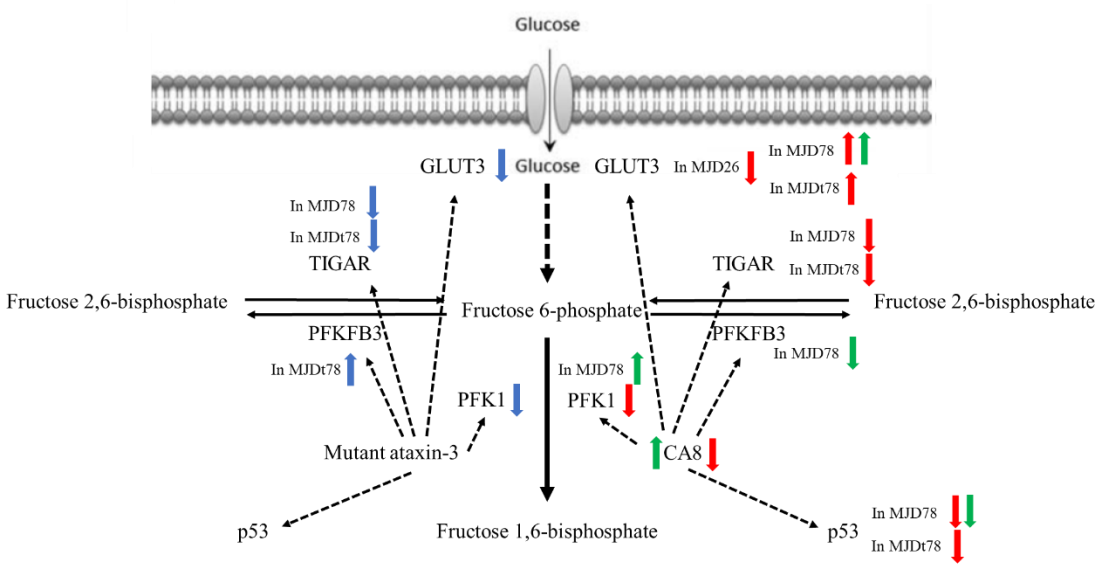

Figure. S6. A model of the effects of CA8 and mutant ataxin-3 in glycolytic pathway of MJD cellular model. In this model, glycolytic enzymes we investigated were showed. Besides reducing glucose uptake, mutant ataxin-3 decreased the protein expression of GLUT3 and PFK1. An increased PFKFB3 was observed in HEK293-MJDt78, and a decreased TIGAR was detected in HEK293-MJD78 and HEK293-MJDt78. In addition, knockdown of CA8 exhibited a significant decrease in PFK1 protein expression. Moreover, a decreased GLUT3 was also observed in HEK293-MJD26-shCA8 while an increased GLUT3 was detected in cells expressing mutant ataxin-3 with down-regulated CA8. Significant increase of GLUT3 and PKF1 were observed in HEK293-MJD78-CA8myc. PFKFB3 was increased only in HEK293-MJD78-CA8myc. P53 was decreased both in HEK293-MJD78 and HEK293-MJDt78 with down-regulated CA8, and was further decreased in HEK293-MJD78-CA8myc. TIGAR was decreased in HEK293-MJD78 and HEK293-MJDt78 with down-regulated CA8. The effects of mutant ataxin-3 were exhibited as blue arrow. The effects of down-regulated CA8 were exhibited as red arrow. The effects of up-regulated CA8 were exhibited as green arrow.

				GLUT3	PFK1	PFKFB3	p53	TIGAR
ataxin-3	26Q	wild-type	-	x	x	x	x	x
			CA8 ↓	↓	↓	N.S.	N.S.	N.S.
			CA8 ↑	N.S.	N.S.			
	78Q	full-length	-	↓	↓	N.S.	N.S.	↓
			CA8 ↓	N.S.	↓	N.S.	↓	↓
			CA8 ↑	↑	↑	↓	↓	N.S.
		truncate	-	↓	↓	↑	N.S.	↓
			CA8 ↓	N.S.		N.S.	↓	↓
			CA8 ↑	N.S.	N.S.	N.S.	N.S.	N.S.

Table. 1. A table illustrated the effects of wild-type (containing 26 polyglutamine repeats) and mutant (containing 78 polyglutamine repeats) ataxin-3 on several glycolytic enzymes mentioned in this study. Up-regulation or down-regulation of CA8 in cells expressing wild-type or mutant ataxin-3 showed different influence on several glycolytic enzymes mentioned in this study. N.S.= non-significant

Titer				
Antibody	**Manufacture**	**Primary antibody**	**Secondary antibody**	**Note**
α tubulin	Novus	1:10000	1:10000	
β actin	Novus	1:10000	1:10000	
Ataxin-3	Millipore	1:3000	1:10000	1^{o}Ab with 2.5% BSA
CA8	Santa Cruz	1:3000	1:10000	1^{o}Ab with 2.5% nonfat milk
GFP	Santa Cruz	1:3000	1:10000	1^{o}Ab with 2.5% nonfat milk
GAPDH	Novus	1:10000	1:10000	
GLUT1	Abcam	1:3000	1:10000	1^{o}Ab with 2.5% BSA
GLUT3	Abcam	1:3000	1:10000	1^{o}Ab with 2.5% BSA
HKI	GeneTex	1:5000	1:10000	
HKII	GeneTex	1:5000	1:10000	
p53	Cell Signaling	1:3000	1:10000	
PFK1	GeneTex	1:5000	1:10000	
PFKFB3	Abcam	1:5000	1:10000	
TIGAR	Santa Cruz	1:3000	1:10000	

Table. 2. A list of antibodies used in this thesis. Manufactures, titers and notes were showed at the top of the table.

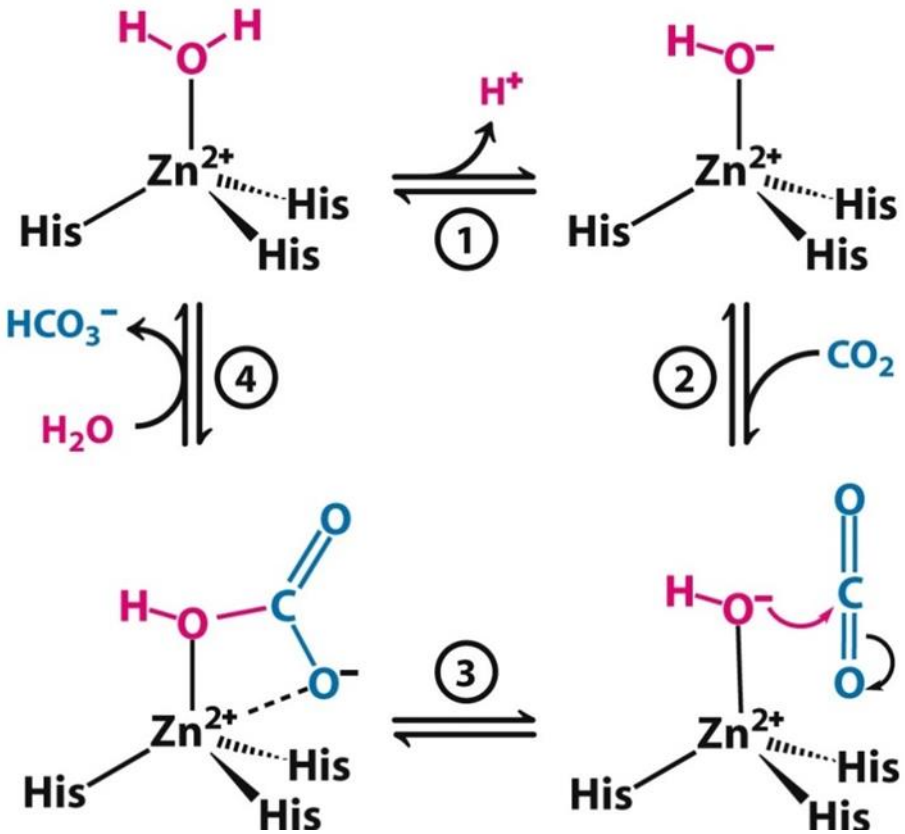

Appendix 1. Carbonic anhydrases have catalytic activity that catalyzes the reversible hydration of carbon dioxide to bicarbonate and protons.

(Adapted from Biochemistry, by Berg, J. M., Tymoczko, J. L., & Stryer, L., 2012, New York, N.Y: W. H. Freeman and Company.)

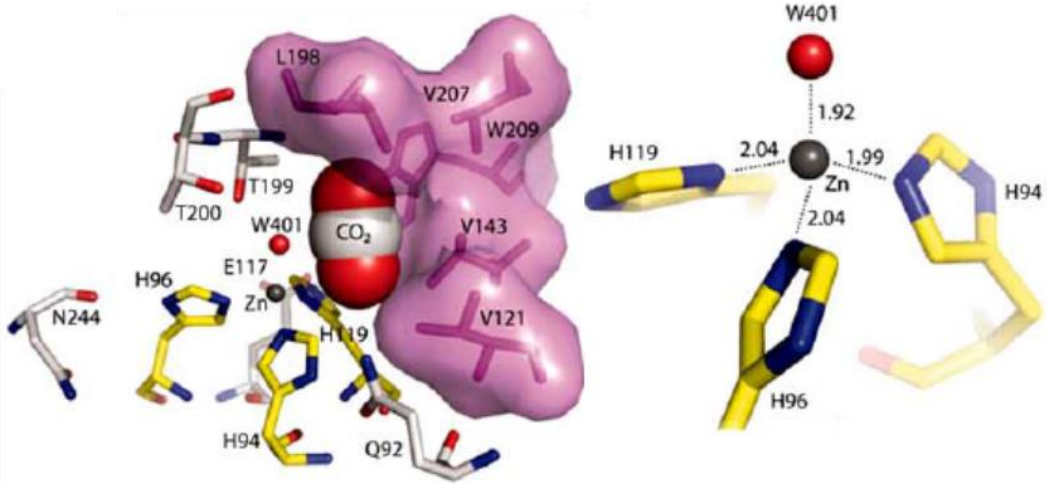

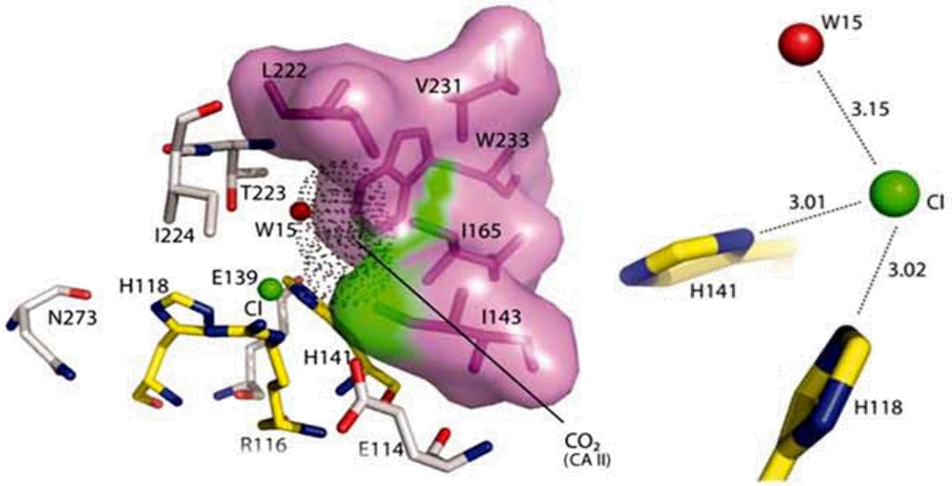

Active site	++	+	+	+ZZ+++Z		+	++		+	++
CA IX	--------TL			--------V	--AF			------AG		
CA XII	-------KNT			--------A	--AY			------NT		
CA XIV	-----T--SA			--------L	---F			------Y		
CA-RP VIII	---D-TI-IYE		R	-----IIIIA				--------G	--L--	
CA-RP X	---TRH-SREE		R	----QIV	--SI-M-I			--YTA-I--		
CA-RP XI	---TRH-SLSE		RL	---QI	--ISI--S			----T--L--		

Appendix 2. (Upper figure) A crystal structure illustrates the protein structure of the functional carbonic anhydrases, the reaction center is surrounded by several zinc binding histidines. (Middle figure) A crystal structure illustrates the protein structure of carbonic anhydrase VIII, the reaction center is lack of one zinc binding histidine, thus cannot bind zinc ion. (Lower figure) CA8, 10, and 11 do not have the enzymatic activity due to lack of the important zinc binding histidine residues

(Modified from "Crystal structure of human carbonic anhydrase-related protein VIII reveals the basis for catalytic silencing," by Picaud SS, 2009, Proteins, 76, p. 510, and from "cDNA sequence of human carbonic anhydrase-related protein, CA-RP X: mRNA expressions of CA-RP X and XI in human brain," by Okamoto N, 2001, Biochim Biophys Acta, 1518, p. 313.)